Cellular studies of the two main isoforms of human D-aspartate oxidase

Valentina Rabattoni[1], Loredano Pollegioni[1], **Gabriella Tedeschi[2], Elisa Maffioli[2],** Silvia Sacchi[1*]

[1]"The Protein Factory 2.0", Dipartimento di Biotecnologie e Scienze della Vita, Università degli studi dell'Insubria, via J. H. Dunant 3, 21100 Varese, Italy

[22]DIMEVET-Dipartimento di Medicina Veterinaria, Università degli Studi di Milano, via Celoria 10, 20122 Milano, Italy

Keywords: D-aspartate**, ~~enzyme isoforms,~~** cellular stability, protein degradation, **neurotransmission,** flavoproteins

Running Title: Properties of human D-aspartate oxidase isoforms

Abbreviations

D-aspartate oxidase (DASPO), D-amino acid oxidase (DAAO), human D-aspartate oxidase (hDASPO), D-aspartate (D-Asp), D-serine (D-Ser) N-methyl-D-aspartate receptors (NMDAR), cycloheximide (CHX), chloroquine (CQ), benzyloxycarbonyl-L-leucyl-L-leucyl-L-leucinal (MG132); ubiquitin-proteasome system (UPS).

*Corresponding author: Silvia Sacchi – Dipartimento di Biotecnologie e Scienze della Vita, Università degli Studi dell'Insubria, via J.H. Dunant 3, 21100 Varese, Italy.

E-mail address: silvia.sacchi@uninsubria.it

Abstract

Human D-aspartate oxidase (hDASPO) is a FAD-dependent enzyme responsible for the degradation of D-aspartate (D-Asp). In **the** mammalian central nervous system D-Asp behaves as a classical neurotransmitter, ~~**being able to activate presynaptic AMPA and mGluR5 receptors and acting as an agonist of N-methyl-D-aspartate receptors. This D-amino acid**~~ is thought to be involved in neural development, brain morphology and behavior, and appears to be entailed in several pathological states, such as schizophrenia and Alzheimer's disease. Apparently, the human *DDO* gene produces alternative transcripts encoding for three putative hDASPO isoforms, constituted by 341 (the "canonical" form), 369 and 282 amino acids. Despite the increasing interest in hDASPO and its physiological role, ~~**have only been partially characterized and**~~ little is known about **the different isoforms**. Here, **the additional N-terminal peptide present in the hDASPO_369 isoform only has been identified in hippocampus of Alzheimer's disease female patients, while peptides corresponding to the remaining part of the protein were present in samples from male and female** healthy controls and Alzheimer's disease patients**. The hDASPO_369 isoform was largely expressed in *E. coli* as insoluble protein, this hampering its biochemical characterization. Anyway,** we generated U87 human glioblastoma cell clones stably expressing hDASPO_341 and, for the first time, hDASPO_369 isoforms**: the latter protein showed a lower expression compared to the canonical isoform. Both protein isoforms** are active (**showing similar kinetic properties**), localize to the peroxisomes, are very stable (a half-life of approximately 100 hours has been estimated) and **are** primarily degraded through the ubiquitin-proteasome system. These studies shed light on the properties of hDASPO isoforms with the final aim to clarify the mechanisms controlling brain levels of the neuromodulator D-Asp.

Introduction

The FAD dependent flavoenzyme D-aspartate oxidase (DASPO or DDO, **EC 1.4.3.1**) was first identified in the '50s in rabbit kidney and liver [1] and now it is known to be widely present in eukaryotes, ranging from fungi to humans [2]. In mammals, the enzyme is primarily involved in the catabolism of acidic D-amino acids **and** the best substrate is D-aspartate (D-Asp). DASPO catalyzes their oxidative deamination into the corresponding α-ketoacids, along with the production of hydrogen peroxide and ammonia [3]. Neutral and basic D-AAs are similarly deaminated by the homologous flavoenzyme, D-amino acid oxidase (DAAO, **EC 1.4.3.3**) [4].

In mammals, free D-Asp has been reported to play different roles: in the endocrine system it modulates steroidogenesis and the synthesis and release of several hormones [5-8], while in the central nervous system it stimulates mGlu5 and presynaptic AMPA receptors [9, 10], as well as N-methyl-D-aspartate receptors (NMDAR), acting as agonist [11]. In the brain D-Asp is abundant during embryonic and perinatal phases and drastically decreases later on [7, 12]. This peculiar temporal distribution pattern is due to the concomitant onset of DASPO expression and activity, mainly observed in neurons [12, 13]. D-Asp has been proposed as a signaling molecule involved in neural development, brain morphology and behavior, and the postulated role of DASPO in strictly regulating its levels has been strengthened [11, 14, 15].

In this regard, several studies performed in animal models demonstrated that the persistent deregulation of D-Asp levels causes age-dependent effects: an improvement of spatial memory and cognitive abilities in young individuals is followed by a rapid deterioration of learning and memory, leading to precocious brain aging [16, 17]. A protective role of DASPO has been proposed: the enzyme would prevent NMDAR hyper-stimulation through the strict regulation of postnatal brain levels of D-Asp.

Despite the increasing interest in hDASPO properties and physiological role, little is known about ~~the~~ processes involved in the regulation of its activity at the cellular level. Notably, the UniProtKB

database reports three different isoforms of hDASPO (identifier **Q99489**) encoded by alternative transcripts of the human *DDO* gene: i) isoform 1 (hDASPO_341, 341 amino acids), referred to as the "canonical isoform", is homologous to the single protein form in rodents; ii) isoform 2 (hDASPO_282), apparently originated by alternative splicing of the transcript, whose sequence is identical to the hDASPO_341 one but lacks of 59 residues in the central region (**residues** 95-153 in the canonical isoform); iii) isoform 3 (hDASPO_369), which appears highly conserved in primates, is characterized by the presence of 28 additional N-terminal residues, probably due to the recognition of an upstream alternative start codon **(Suppl. Fig. 1)**. The shorter protein isoforms were produced in *E. coli* [18, 19], while the longer one has never been expressed. Notably, the recombinant deleted hDASPO_282 form was **largely** produced as inclusion bodies [19]. The three-dimensional structure of human DASPO_341 (hDASPO, PDB entry code **6RKF**), and an extensive characterization of its biochemical properties, have been recently published [18].

In order to look deep inside into the role of the two main hDASPO isoforms, here we investigated by a proteomic approach the presence of hDASPO in hippocampus of male and female healthy subjects and Alzheimer's disease (AD) patients: the hDASPO_369 isoform was identified exclusively in the hippocampus of female AD patients. The functional properties, the degradation kinetics and the mechanisms involved in protein turnover **were investigated** by ectopically expressing hDASPO_341 and hDASPO_369 isoforms in the U87 human glioblastoma cell line. This study demonstrated that both hDASPO isoforms are active (thus, able to control D-Asp cellular level), are highly stable and mainly degraded through the ubiquitin-proteasome system.

Results

Identification of hDASPO isoforms in human hippocampus by nLC-MS/MS

Hippocampus is a brain area relevant for the formation and consolidation of memory and it is specifically vulnerable to damage at early stages of AD. We investigated the presence of

hDASPO in hippocampus samples from male and female healthy controls and AD patients by using a nLC-MS/MS approach. The results, briefly summarized in Table 1 and Supplementary Fig. 1, clearly show that the N-terminal peptide (exclusively present in the hDASPO_369 isoform) was identified in female AD samples only (1-MRPARHWETR-10 peptide) while peptides covering the regions common to both 341 and 369 isoforms were identified in all samples.

Expression of hDASPO_369 in E. coli cells

The synthetic gene encoding the His-tagged hDASPO_369 was subcloned into the pET11a expression vector and the protein was expressed in *E. coli* BL21(DE3) LOBSTR cells using the procedure reported for hDASPO_341 [18]. Differently from the latter, the hDASPO_369 isoform was largely expressed as inclusion bodies. The use of the ArcticExpress (DE3) *E. coli* strain (expressing the "cold adapted" chaperons Cpn10 and Cpn60) and of conditions favoring heterologous proteins folding, i.e. incubation at 13 °C for 24 hours after adding the inducer, yielded a very low amount of soluble recombinant protein (not shown). The purification of hDASPO_369 from the crude extract by HiTrap chelating chromatography yielded ≤ 0.06 mg/liter of fermentation broth, an amount inadequate for performing kinetic and spectral studies.

Solubilization and refolding of hDASPO_369 from inclusion bodies was attempted using different procedures and conditions (Supplementary Table 1): once more we failed in obtaining a significant amount of the soluble protein isoform. In line with protein expression results, bioinformatics evaluation of protein solubility by four different methods predicted a significantly lower solubility for the longer isoform compared to the canonical hDASPO_341 isoform (Supplementary Table 2).

Expression of hDASPO isoforms in U87 cells

Expression plasmids were generated by subcloning the sequences encoding the hDASPO_341 and hDASPO_369 isoforms in the pcDNA3 vector. The corresponding DNA fragments were produced by PCR amplification of hDASPO cDNA using different 5'-primers designed to anneal to the alternative ATG sites and to insert, beside two unique restriction sites, a 5'-sequence coding for 3 copies of the FLAG epitope (N-terminal 3XFLAG). The generated pcDNA3_3XFLAG-hDASPO_341 and pcDNA3_3XFLAG-hDASPO_369 expression constructs were used to transfect human glioblastoma U87 cells and cell clones stably expressing the long or the short hDASPO isoform were selected.

Western blot analysis on selected cell clones confirmed the expression of both hDASPO_341 and hDASPO_369 isoforms (Fig. 1A), although the longer one at a 4-fold lower level (Fig. 1B). The Western blot analysis of U87 3XFLAG-hDASPO_341 cell lysates with the anti-hDASPO antibody recognized a band at the expected molecular mass (≈ 42.0 kDa, corresponding to 3XFLAG-hDASPO_341) and a band at ≈ 37.0 kDa. On the other hand, the same analysis performed on U87 3XFLAG-hDASPO_369 cell lysates revealed the presence of three bands: in addition to the 37 kDa band, signals at ≈ 40.5 and 44.0 kDa were also apparent (Fig. 1A). In both cell clones, the band at the lowest molecular mass, ≈ 37.0 kDa, should correspond to an aspecific signal since it was also present in control samples (U87 untransfected cells). Based on the molecular mass, the bands at ≈ 40.5 and 44 kDa correspond to untagged hDASPO_341 and 3XFLAG-hDASPO_369 isoforms, respectively: both bands were recognized by the anti-hDASPO antibody, while only the latter one was detected by the anti-FLAG antibody (not shown). Therefore, U87 cells transfected with the pcDNA3_3XFLAG-hDASPO_369 construct expressed both protein isoforms at comparable levels (Fig. 1B).

The identity of the expressed protein isoforms in the U87 3XFLAG-hDASPO_369 cells was determined using immunoprecipitation (IP) experiments. In **detail**, two consecutive IP rounds were carried out: the first one using the whole cell extract and the anti-FLAG M2 affinity resin; the second using the obtained post-IP sample and the anti-hDASPO antibody crosslinked to Dynabeads

Protein G. Western blot analyses of the immunoprecipitated samples confirmed that both 3XFLAG-hDASPO_369 and the untagged hDASPO_341 isoforms were present in the cell extract (Fig. 1C,D). The untagged hDASPO_341 originates by the translation of the hDASPO_369 encoding transcript at an alternative, down-stream starting codon.

hDASPO isoforms are active

A sensitive fluorimetric assay using the Amplex UltraRed reagent and based on the detection of hydrogen peroxide produced by hDASPO in the presence of a saturating concentration of the substrate D-Asp (16.7 mM) [20] was used to assess the enzymatic activity of the two protein isoforms. 3XFLAG-hDASPO_369 and 3XFLAG-hDASPO_341 were immunoprecipitated from the corresponding cell lysates using an anti-FLAG M2 affinity resin, and the activity assays were performed on the purified protein form. The specific activity of the two hDASPO isoforms, calculated by normalization for the amount of the immunoprecipitated protein in each well, as assessed by Western blot analysis, were very similar (34.4 ± 7.6 and 38.7 ± 6.9 U/mg for the 3XFLAG-hDASPO_369 and 3XFLAG-hDASPO_341 isoform, respectively) and **slightly lower** than the value determined for the recombinant purified hDASPO (55.1 ± 3.9 U/mg). **Immunoprecipitated samples were also used to evaluate the apparent kinetic properties on D-Asp: the two isoforms show similar k_{cat} and K_m values (i.e. 27.8 ± 0.6 and 27.4 ± 1.3 s^{-1} and 0.44 ± 0.04 and 0.29 ± 0.07 mM for hDASPO_369 and hDASPO_341, respectively). This method gave for the recombinant hDASPO a k_{cat} of 76.4 ± 7.1 s^{-1} and a K_m of 2.04 ± 0.60 mM which are comparable to the previously reported values (81.3 ± 1.5 s^{-1} and 1.05 ± 0.06 mM) [18].**

hDASPO expression controls cellular levels of D-aspartate

HPLC analysis of amino acid enantiomers showed that the ectopical expression of the 3XFLAG-hDASPO_341 isoform deeply affects D-Asp cellular content: basal D-Asp levels (0.044 ± 0.006

nmol/mg proteins in control cells transfected with the pcDNA3 empty vector) were fully depleted in 3XFLAG-hDASPO_341 expressing cells (Fig. 2A), whereas the L-enantiomer content was unaffected (5.97 ± 1.25 and 6.67 ± 1.14 nmol/mg proteins in transfected and control cells, respectively). Accordingly, a dramatic decrease of the D-Asp/total Asp ratio in the transfected cells was also evident (Fig. 2A, right panel). On the other hand, serine (Ser) enantiomers levels appeared only marginally altered by 3XFLAG-hDASPO_341 expression: L-Ser content slightly increased (12.7 ± 5.2 and 8.2 ± 0.9 nmol/mg proteins in transfected cells compared to controls, respectively) and the D-Ser/total Ser ratio remained unchanged (Fig. 2B).

hDASPO isoforms are peroxisomal enzymes

The peroxisomal targeting of hDASPO should be determined by the non-canonical C-terminal PTS1 sequence (-SNL). The subcellular localization of hDASPO_369 and hDASPO_341 isoforms was verified by immunostaining and confocal analysis performed on the stable clones expressing the two protein isoforms and on U87 untransfected cells as a control. The ectopically expressed 3XFLAG-hDASPO_369 and 3XFLAG-hDASPO_341 were specifically detected using either the anti-FLAG or the anti-hDASPO antibody (no immunorecognition was observed in control cells, Fig. 3A,D). Both protein isoforms showed a **punctate** distribution within the cells (Fig. 3B,C and E,F) consistent with their targeting to the peroxisomal compartment, as demonstrated by the large overlapping of FLAG immunofluorescence signals to PMP70 ones (red and green channel, respectively; Fig. 3B,C, merge panels). Conversely, no signal overlapping was apparent when the protein isoforms were co-stained with the protein marker recognized by the anti-mitochondria antibody (green and red channel, respectively; Fig. 3E,F, merge panels). In this case we used the anti-hDASPO antibody, which allowed to detect both the 3XFLAG-hDASPO_369 and the untagged hDASPO_341 isoforms expressed by U87 3XFLAG-hDASPO_369 cells: the same **punctate** distribution pattern was evident. Notably, both protein isoforms were not detected in the cytosol, at least at significant levels.

hDASPO isoforms are long-lived proteins

The cellular stability of 3XFLAG-hDASPO_369 and 3XFLAG-hDASPO_341 was investigated by treatment with cycloheximide (CHX), an inhibitor of protein synthesis that prevents translational elongation. Western blot analysis showed only a slight decrease in both the FLAG-tagged hDASPO isoforms abundance during time: about 80% of the initially observed protein isoform was still detectable at 32 hours after the treatment (Fig. 4). Thus, for both proteins, **a** half-life of approximately 100 hours was estimated. Furthermore, the N-terminal 3XFLAG additional sequence did not appear to influence the kinetics of protein degradation, since the same half-life value was also determined for the untagged hDASPO_341 expressed in the U87 cell clones transfected with the pcDNA3_3XFLAG-hDASPO_369 construct (Fig. 4). These results indicated that hDASPO is a long-lived protein, as it was previously reported for hDAAO [21].

hDASPO isoforms are degraded by the ubiquitin-proteasome system

The mechanisms involved in hDASPO degradation were investigated by treating U87 cell clones expressing 3XFLAG-hDASPO_369 or 3XFLAG-hDASPO_341 isoforms with inhibitors of autophagy or of the ubiquitin-proteasome system (blocking the preferential degradation pathway should lead to the accumulation of the protein), upon incubating the cells overnight under starvation conditions (i.e. in culture media containing 1% FBS). Starvation is a physiological stimulus inducing numerous changes within the cell: two out of the major effects are a decreased protein synthesis and the activation of proteolytic pathways [22]; accordingly, under starvation conditions the effect of the inhibitors of protein degradation pathways should be enhanced.

Since autophagy is responsible for cytoplasmic bulk degradation and is thought to be important for the turnover of whole organelles and long-lived proteins [23, 24], we investigated the effect of two autophagy inhibitors, namely chloroquine (CQ, 75 μM) and ammonium chloride (NH_4Cl, 10 mM), on the cellular levels of hDASPO variants. The chosen inhibitors act by different mechanism: CQ

inhibits autophagy mainly by impairing autophagosome fusion with lysosomes, whereas NH_4Cl acts on the proton gradient affecting lysosomal pH and thus the degradative activity of hydrolytic enzymes within this organelle [25, 26]. No difference in the relative abundance of 3XFLAG-hDASPO_369 and 3XFLAG-hDASPO_341 was detected in treated cells compared to controls (Fig. 5A), despite CQ and NH_4Cl treatments were prolonged up to 10 hours, suggesting that they do not affect the turnover of these protein variants. This result was unexpected since hDAAO, which is also targeted to peroxisomes and shares a high degree of sequence identity and enzymatic functionality with hDASPO, **is** primarily degraded by the lysosome/endosome system [21].

The effect of MG132 on hDASPO cellular level was also investigated. This compound acts as a proteasomal inhibitor interacting with the 'chymotrypsin-like' component and blocking one or more peptidases within the 20S proteasome core, without affecting protein-ubiquitinating and -deubiquitinating enzymes [27]. The treatment of stably transfected cells with 25 µM MG132 **led** to the gradual and moderate accumulation of both 3XFLAG-hDASPO_369 and 3XFLAG-hDASPO_341 proteins (Fig. 5B): a 1.6-fold increase at 6-10 hours after treatment was detected for both **i**soforms. This resembles what **was** previously observed for hDAAO (i.e. a 1.5-fold increase) [21], and eventually suggests a slow synthesis of both flavoproteins under starvation conditions. hDASPO_369 and hDASPO_341 behaved again exactly in the same way, indicating that the N-terminal sequence (absent in the shorter isoform) did not affect the degradation mechanism as well as the targeting to, and the recognition by, the ubiquitin-proteasome system (UPS).

Ubiquitination of hDASPO isoforms

hDAAO was demonstrated to form ubiquitin conjugates by *in vitro* and cellular studies, and it was proposed that this signal drives its targeting to the UPS during the protein degradation [21]. *In vitro* ubiquitination experiments were carried out by mixing 5 µg of purified recombinant hDASPO (i.e. hDASPO_341 isoform), 0.6 mg/mL ubiquitin, 5 mM ATP, 1 mM dithiothreitol, 2 mM $MgCl_2$, 1 µM ubiquitin aldehyde (to inhibit deubiquitinating enzymes), 25 µM MG132 (to block the

proteasome degradation activity) and 4 mg/mL U87 cell extract (to provide the components of the UPS). Upon incubation for 60 min at 37 °C, aliquots of the reaction mixtures were analyzed by Western blot. Distinct bands at high molecular mass, corresponding in size to mono- (44.5 kDa), multi- or polyubiquitinated (57.2 – 102 kDa) hDASPO species, were observed, see Fig. 6A: the same bands were absent in control samples (i.e. reaction mixtures prepared by omitting the recombinant hDASPO or ubiquitin). The assay of the enzymatic activity on the same samples (using saturating concentration of substrate and cofactor, i.e. at 15 mM D-Asp and 40 μM FAD) showed no change in hDASPO enzymatic activity (Fig. 6B).

The ubiquitination state of hDASPO isoforms at the cellular level was investigated by **IP** experiments on the U87 cell clones stably overexpressing the hDASPO isoforms and transiently transfected with a FLAG-tagged ubiquitin expression construct. The highest expression level of FLAG-ubiquitin was observed 48 h after transfection with the pCMV-FLAG-ubiquitin vector (data not shown). Accordingly, cells were treated 48 hours after transfection **with 25 μM MG132 and** collected 6 hours after treatment: cell lysates were **then** immunoprecipitated with the anti-FLAG M2 affinity resin. Western blot analysis indicated that both hDASPO isoforms have been modified by ubiquitin: an intense anti-hDASPO signal was detected at high molecular mass in the immunoprecipitated protein samples from both 3xFLAG-hDASPO_369 and 3XFLAG-hDASPO_341 expressing cells (Fig. 7, lanes 1 and 4, respectively). The detected signal is specific for the ubiquitin conjugated protein isoforms since it is absent in U87 control cells transiently transfected with the FLAG-ubiquitin expression vector and treated with MG132 (Fig. 7, lane 7). Notably, an anti-hDASPO immunorecognition signal was also evident in **U87 cell clones expressing** 3xFLAG-hDASPO_369 **or** 3XFLAG-hDASPO_341 not treated with the proteasome inhibitor or not overexpressing FLAG-ubiquitin and subjected to MG132 treatment (Fig. 7, lanes 2-3 and 5-6). Altogether, both hDASPO isoforms are polyubiquitinated at the cellular level.

Discussion

In the brain of mammals, D-Ser is critical for neurotransmission since it modulates the activation state of NMDAR by acting as the main endogenous co-agonist of this receptor. For this reason its synthesis, transport and degradation processes have been characterized in depth [28-30]. A second D-amino acid, D-Asp, is also involved in neurotransmission, due to its relatively high affinity for the glutamate binding site of NMDAR. D-Asp shows a peculiar temporal occurrence in the brain, with its levels peaking during early embryonic development and drastically falling after birth [6, 7, 15]: the regulation of D-Asp levels is mainly exerted by the catabolic activity of hDASPO. This peroxisomal flavoenzyme, together with hDAAO (which is responsible for the selective degradation of D-Ser) [31], belongs to the amino acid oxidase family of flavoproteins. Despite the two orthologue flavoproteins **sharing a** high sequence identity and a similar overall tertiary structure, hDASPO and hDAAO profoundly differ in their quaternary structure, cofactor binding affinity, kinetic properties and mechanisms [18]. These findings indicate that they should regulate the brain levels of D-Asp and D-Ser differently.

Interestingly, three different isoforms of hDASPO can be identified in the UniProtKB database: hDASPO_341 (37.5 kDa, the "canonical" protein isoform), hDASPO_282 (30 kDa), and hDASPO_369 (41 kDa). We focused on the hDASPO_341 and hDASPO_369 isoforms. **For the first time, we demonstrated that the latter longer isoform is expressed in the hippocampus of female AD patients (Table 1). This is an intriguing observation that pushed the investigation of the biochemical properties of the two hDASPO isoforms. Unluckily, the recombinant hDASPO_369 cannot be characterized since it is largely produced in *E. coli* cells as an insoluble protein.** Both protein isoforms were expressed in U87 cells after transfection: the 3XFLAG-hDASPO_369 isoform was expressed at a significantly lower level (Fig. 1). Notably, the cells transfected with the pcDNA3_3XFLAG-hDASPO_369 construct produced both the long and the untagged short protein isoforms at similar levels (Fig. 1B), suggesting that the translation of hDASPO_369 encoding transcript can occur from the alternative starting codon at a similar frequency. Notably, both hDASPO_369 and hDASPO_341 isoforms were efficiently targeted to the

peroxisomes **and showed similar kinetic properties on D-Asp**. Furthermore, the ectopically expressed hDASPO_341 isoform fully depleted D-Asp cellular pool while not significantly affected the levels of D-Ser and the corresponding L-enantiomers (Fig. 2).

Similarly to the homologous hDAAO protein [21], both hDASPO isoforms were highly stable proteins and likely characterized by a slow cellular turnover: their estimated half-life was ≈100 hours (Fig. 4), even higher than that for catalase (≈30 hours) [32]. This value is in line with the peroxisomal localization of hDASPO isoforms, since most data indicate a peroxisomal half-life of around 2 days [33]: peroxisomes are thought to be mainly degraded by autophagy, with a process mediated by p62 and LC3-II named pexophagy [33] that can be upregulated in response to different stresses, such as nutrient starvation. Accordingly, ectopically expressed hDAAO accumulated in U87 cells in this condition upon blocking the lysosome/endosome pathway [21]. On the contrary hDASPO_341 and hDASPO_369 isoforms were degraded by the UPS.

Actually, *in vitro* and cellular studies revealed that hDASPO isoforms can be ubiquitinated (Fig. 6A and 7), a modification that did no**t a**ffect the enzymatic activity (Fig. 6B). This observation suggests that (poly)ubiquitin conjugation represents the cellular signal that triggers the targeting of hDASPO to the UPS and thu**s t**hat the modified flavoenzyme should be retrotraslocated to the cytoplasm for degradation. It is known that excessive peroxisomal matrix proteins may be exported to the cytosol where they are degraded by cytosolic proteases or the proteasome [34]. In this context, it is noteworthy that peroxisomal membrane receptors involved in the import apparatus (e.g. Pex5p, Pex7p, and Pex20p) can also be degraded by the UPS [34] and that the ubiquitination pattern controls their targeting: when the export is impaired, they are polyubiquitinated and extracted from the peroxisomal membrane for degradation by the UPS, a process called RADAR (Receptor Accumulation and Degradation in the Absence of Recycling) [35]. Since the RADAR quality control pathway is most likely conserved in mammals, it is tempting to speculate that this mechanism is involved in the regulation of hDASPO cellular levels.

We can conclude that the additional N-terminal sequence in the long hDASPO isoform does not affect the enzyme functionality, subcellular localization, half-life and degradation pathway. **The main difference is a lower solubility for the longer isoform and its selective expression in the hippocampus of AD female patients.** In order to understand how the cellular levels of D-Asp are controlled, further studies will focus on the effects due to post-translational modifications and ligand interactions on hDASPO isoforms **under physiological and pathological conditions**.

Materials and Methods

Expression vectors

The cDNA encoding hDASPO was purchased as a full ORF clone from the PlasmID Repository at Harvard Medical School (HsCD00335325 pCMV-SPORT6) and amplified with primers, reported in Supplementary Table 3, specifically designed to obtain the two different isoforms with three copies of the FLAG (DYKDDDDK) epitope fused to the N-terminal end. These cDNAs were then subcloned into pcDNA3 vector, and the resulting constructs were confirmed by automated sequencing. The pCMV-FLAG-ubiquitin vector for the expression of N-terminal FLAG tagged human ubiquitin, was kindly provided by professor Herman Wolosker (Technion – Israel Institute of Technology, Haifa, Israel).

For *E. coli* expression, the synthetic cDNA coding for hDASPO_369 (produced by GeneArt®) was designed to contain an N-terminal 6xHis encoding sequence and was optimized in the codon usage [18]. It was amplified by PCR using the oligos reported in Supplementary Table 3 and subcloned in the pET11a expression vector (Novagene, Merck KGaA) using the inserted restriction sites.

E. coli expression systems

Heterologous expression of hDASPO_369 in *E. coli* cells was performed in BL21(DE3) LOBSTR (Kerafast Inc.) and ArcticExpress (DE3) (Agilent Technologies) cells. In BL21(DE3) LOBSTR cells hDASPO_369 expression was induced as previously reported for the canonical

DASPO_341 isoform [18], while the conditions indicated by the supplier were adopted for protein expression in ArcticExpress (DE3) *E. coli* cells. Briefly, cells grown at 30 °C under shaking (OD_{600nm} = 0.7) were added of either 1 mM or 0.1 mM IPTG and harvested after a 24 hours incubation at 13 °C under shaking. The recombinant protein expression levels were evaluated by SDS-PAGE; both the soluble and insoluble fractions of cell lysates were analyzed.

Attempts to purify the soluble His-tagged hDASPO_369 from the crude extracts were carried out using a HiTrap chelating column (GE Healthcare) as reported in [18].

Refolding and purification of insoluble hDASPO_369

After cell lysis and centrifugation, the insoluble fraction of the *E. coli* cell extracts was recovered and washed twice in 20 mM Tris-HCl pH 8.0, 2 M urea, 0.5 M NaCl, 2% (v/v) Triton X-100. Different refolding procedures were used: i) the column-refolding of inclusion bodies solubilized in 20 mM Tris-HCl pH 8.0, 6 M guanidine hydrochloride, 0.5 M NaCl, 5 mM imidazole, and 1 mM 2-mercaptoethanol, loaded on a HiTrap Chelating HP column, refolded using a linear gradient from 6 to 0 M of urea and from 0 to 40 µM FAD and then eluted with 20 mM Tris–HCl pH 8.0, 0.5 M NaCl, at increasing concentration of imidazole (100, 250 and 500 mM); ii) the solubilization of inclusion bodies as above, followed by dialysis to remove the chaotropic agent; iii) the solubilization of inclusion bodies in 50 mM Tris-HCl pH 8.0, 2 M urea and 6 M *n*-propanol followed by a refolding step by dialysis to remove urea and *n*-propanol. At the end of the procedures, samples were centrifuged (at 39000 g for 30 min at 4 °C) and the soluble and insoluble fractions analyzed by SDS-PAGE.

Cell culture and transfection

The U87 human glioblastoma cells (ATCC) were maintained in Dulbecco's Modified Eagle Medium (DMEM) supplemented with 10% fetal bovine serum (FBS), 1 mM sodium pyruvate, 2 mM L-glutamine, 2.5 µg/mL amphotericin B and 1% penicillin/streptomycin (all from Euroclone) at 37 °C in a 5% CO_2 incubator and transfected using the FuGENE HD transfection reagent (6 µL;

Roche) and 2 μg of pcDNA3_3XFLAG-hDASPO_341 or -hDASPO_369 constructs. Stable clones were selected adding 0.4 mg/mL G418 to the growth medium. To perform ubiquitination studies, U87 3XFLAG-hDASPO_341 or -hDASPO_369 cells were transiently transfected with 2 μg of the pCMV-FLAG-ubiquitin vector. For immunolocalization studies, 10^4 U87 3XFLAG-hDASPO_341, 3XFLAG-hDASPO_369 cells and U87 control cells were seeded onto previously gelatinised coverslips (diameter 12 mm, Thermo Scientific). At 24 h after seeding, cells were extensively washed with PBS (10 mM dibasic sodium phosphate, 2 mM monobasic potassium phosphate, 137 mM NaCl, 2.7 mM KCl, pH 7.4) and fixed with 4% *p*-formaldehyde for 10 min at room temperature.

To evaluate the stability of hDASPO_341 and _369 isoforms and assess their rate of degradation, U87 3XFLAG-hDASPO_341 and -hDASPO_369 cells were seeded in 6-well plates ($2.7x10^5$ cells/well) and treated up to 32 hours with cycloheximide (CHX, 100 μg/mL; Sigma), a potent inhibitor of protein synthesis, and collected at different times for Western blot analysis [21]. Changes in hDASPO isoforms cellular levels were determined by densitometric analysis upon acquisition with an Odyssey Fc Imaging System (LI-COR Biosciences). Data were fit to a single exponential decay equation to estimate the half-life.

Processes involved in hDASPO degradation were investigated by treating the cell clones expressing the two protein isoforms with specific inhibitors of autophagy/lysosomal pathway or the ubiquitin-proteasomal system (UPS) [21]. After seeding, the cells were grown overnight under starvation conditions (DMEM supplemented with 1% FBS) and then the lysosomal hydrolase inhibitors chloroquine (CQ, 75 μM; Sigma) or NH_4Cl (10 mM; Sigma) or the proteasomal inhibitor benzyloxycarbonyl-L-leucyl-L-leucyl-L-leucinal (MG132, 25 μM; Sigma) were added. At different time points (up to 10 hours), cells were collected by trypsinization and the protein levels analyzed by Western blot. Starvation conditions have been used to maximize the effect of inhibition of the degradation pathways, as previously reported [21, 36].

Immunoblot

For Western blot analysis, stably transfected or control cells were resuspended in sample buffer (12.5 mM Tris-HCl, pH 6.7, 3% SDS, 5% glycerol and 62.5 mM dithiothreitol) to have 5000 cells/μL and 10 μL of each sample was subjected to SDS-PAGE. Proteins were then transferred to polyvinylidene difluoride membranes (Immobilon-P, Millipore) and saturation of aspecific sites was performed by incubation (2 h at room temperature or overnight at 4 °C) in a blocking solution containing 4% dried milk in Tris-buffered saline (TBS; 10 mM Tris–HCl pH 8.0, 0.5 M NaCl) with the addition of 0.1% Tween-20 (TBST). Membranes were then incubated with primary antibodies at room temperature for 1.5 h, extensively washed in TBST and then incubated for 1 h at room temperature with specific peroxidase-conjugated immunoglobulins. The immunoreactivity signals were detected by enhanced chemiluminescence (WESTAR ETA C Ultra 2.0 reagents; Cyanagen) using the Odyssey Fc Imaging System (LI-COR Biosciences).

The primary antibodies used were: rabbit polyclonal anti-hDASPO (1:1000, Davids Biotechnologie); rabbit polyclonal anti-FLAG (1:500, Sigma); mouse monoclonal anti-β-tubulin (1:2000, Thermo Scientific).

The different immunorecognition signals in cell lysates were measured using the Image Studio Lite Software (LI-COR Biosciences). The intensity values of the bands detected by the anti-hDASPO antibody were normalized to the values of the anti-β-tubulin ones. After normalization, the ratio of the intensity signals corresponding to treated and control cells, collected at the same incubation time, **were** calculated.

Immunostaining and confocal analysis

In order to analyze the subcellular localization of the hDASPO isoforms, p-formaldehyde fixed U87 3XFLAG-hDASPO_341, 3XFLAG-hDASPO_369 and U87 control cells were permeabilized and the unspecific binding sites were blocked by incubation in PBS supplemented with 0.2% Triton X-100 and 4% horse serum. DASPO isoforms were subsequently stained using rabbit polyclonal anti-hDASPO (1:500, Davids Biotechnologie) and mouse monoclonal anti-FLAG antibody (1:500,

Invitrogen); peroxisomes and mitochondria were stained by rabbit polyclonal anti-PMP70 (peroxisomal membrane protein 70, 1:500, Sigma) and mouse monoclonal anti-mitochondria antibody (1:500, Millipore). Cells were incubated with primary antibodies overnight at 4 °C and, after extensive washing in PBS supplemented with 1% horse serum, with anti-rabbit Alexa 488 and anti-mouse Alexa 546 antibodies (1:1000, Molecular Probes) diluted in PBS, 0.1% Triton X-100, and 1.5% horse serum.

Immunostained coverslips were imaged using an inverted laser scanning confocal microscope (TCS SP5, Leica Microsystems), equipped with a 63.0 × 1.25 NA plan apochromatic oil immersion objective. Confocal image stacks (5 sections with optimized thickness) were acquired using the Leica TCS software with a sequential mode to avoid interference between each channel due to spectral overlap and without saturating any pixel.

Immunoprecipitation

To determine the specific activity of 3XFLAG-hDASPO_341 and 3XFLAG-hDASPO_369, the enzymes were purified from cell extracts by immunoprecipitation (IP) using anti-FLAG M2 Affinity resin (Sigma). Briefly, U87 cell clones stably expressing the two isoforms were suspended in ice-cold lysis buffer (50 mM sodium phosphate pH 8.0, 0.7 µg/mL pepstatin, 1 µg/mL leupeptin, 5 µM FAD, 0.1% ethanol, 1 mg/mL DNAse) and sonicated. The cell lysates were then centrifuged at 13000 g for 30 min at 4 °C; the protein concentration of the supernatant (Pre-IP sample) was quantified using the Bradford reagent (Sigma). A volume of sample corresponding to 0.5 mg (or 2 mg for U87 3XFLAG-hDASPO_369 cells) of total protein was subjected to IP using 40 µL of anti-FLAG M2 Affinity resin and incubated overnight at 4 °C under constant rotation. The sample was then centrifuged at 8000 g for 1 minute and the supernatant (Post-IP sample) was stored for Western blot analysis. The pelleted resin and the bound flagged protein were resuspended in 50 µL of lysis buffer for the subsequent activity measurements (IP sample).

To confirm the identity of the protein forms expressed in cells transfected with the pcDNA3_3XFLAG-hDASPO_369 vector, after a first IP using the whole cell extract and the anti-

FLAG M2 Affinity resin, a second IP was performed using the anti-hDASPO antibody. In details, after the removal of flagged proteins, the obtained post-IP sample was incubated with 50 µL of Dynabeads Protein G (Invitrogen) previously cross-linked to 10 µg of rabbit anti-hDASPO antibody (Davids Biotechnologie) using dimethyl pimelimidate (DMP), and the procedure previously reported [21]. After an overnight incubation at 4 °C with rotation, the supernatant (post-IP sample) was collected by separating the beads on the magnet; beads were extensively washed with lysis buffer, suspended in 50 µL of non-reducing SDS-PAGE sample buffer (IP sample) and boiled. SDS-PAGE and Western blot analyses were performed using an amount of pre-IP and post-IP samples corresponding to 20 µg of total protein and 10 µL of the IP samples.

DASPO activity assay ***and kinetic measurements***

hDASPO activity was assayed on total cell lysates and on hDASPO isoforms purified by IP using the Amplex UltraRed assay kit (Invitrogen) based on the detection of H_2O_2 by the peroxidase-mediated oxidation of the fluorogenic Amplex UltraRed Dye [20]. Cells were suspended in ice-cold 50 mM sodium phosphate buffer, pH 8.0, containing 0.7 µg/mL pepstatin, 1 µg/mL leupeptin, 5 µM FAD, 0.1% ethanol, and 1 mg/mL DNAse, sonicated, and centrifuged at 13000 g for 30 min at 4 °C. The protein concentration in the supernatant was quantified using the Bradford assay (Sigma)**.** The IP samples were obtained as reported above. A volume of cell extract corresponding to 2.5 and 5 µg of total protein content or to 2 and 3 µL of the resuspended IP samples were aliquoted in black 96-well plates and added **to** lysis buffer to a final volume of 100 µL. Then 50 µL of the activity assay solution (55 µM Amplex UltraRed, 0.15 U/mL horseradish peroxidase, 7.5 mM NaN_3, 50 mM D-Asp and 15 µM FAD in 50 mM sodium phosphate buffer, pH 8.0) were added to each well. The fluorescence measurements (excitation at 535 nm and emission at 590 nm) were recorded at 25 °C every 5 minutes for a total of 30 minutes and values were corrected for controls wells (without the samples) to subtract background signal. As a positive control, different amounts of the recombinant purified enzyme (0.0025-0.1 milliunit range) were assayed in parallel. The assay specificity was assessed using lysates of control U87 cells stably transfected with the empty

pcDNA3 vector, as a negative control, and adding 2 mM 5-aminonicotinic acid (an inhibitor of hDASPO, K_i = 3.8 µM) [37] to hDASPO expressing cells.

The concentration of H_2O_2 in the wells was determined using a calibration curve (0.25–7.5 µM H_2O_2). hDASPO specific activity (µmol/min/mg) was then calculated **by** dividing the nanomoles of H_2O_2 produced in a minute by the milligrams of enzyme present in the samples, determined in turn by Western blot and densitometric analysis, using a calibration curve prepared **by** analyzing known amounts of the recombinant purified hDASPO.

The apparent kinetic parameters of hDASPO isoforms on D-Asp were determined using the same assay, after the purification of the isoforms by IP, and were calculated according to a Michaelis–Menten equation using the initial velocity values determined at increasing substrate concentrations (0.4-16 mM range). As a positive control, a fixed amount of the recombinant hDASPO (corresponding to 0.07 mU) was assayed.

In vitro ubiquitination

Recombinant hDASPO was expressed in *E. coli* BL21(DE3) LOBSTR host cells (Novagen) and purified as reported in [18]. *In vitro* ubiquitination experiments were carried out using 2 and 5 µg of hDASPO, incubated with 0.6 mg/mL ubiquitin, 1 µM ubiquitin aldehyde, 5 mM ATP, 25 µM MG132, 1 mM dithiothreitol, 2 mM $MgCl_2$ and 4 mg/mL U87 cell extract in 20 mM Tris-HCl (pH 8.0), in a total volume of 60 µL, at 37 °C for 60 min. Controls were performed by omitting ubiquitin or hDASPO in the mixture. The ubiquitin-hDASPO conjugates were resolved by SDS-PAGE and analyzed by Western blot using rabbit anti-hDASPO antibody. For preparation of U87 cell extract, the cells were collected, resuspended (10^7 cells/mL) in lysis buffer (20 mM Tris-HCl pH 8.0, 1 mM dithiothreitol, 5 mM KCl, 2 mM $MgCl_2$, 2 µM leupeptin, 1 µM pepstatin, 50 µM phenylmethanesulfonyl fluoride, 25 µM MG132) and subjected to sonication (three cycles of 10 s each). The cell lysate was cleared by centrifugation (see above).

Before and after *in vitro* modification, recombinant hDASPO activity was assayed in 100 mM disodium pyrophosphate buffer (pH 8.3), 40 µM FAD using 15 mM D-Asp as substrate, at 25 °C

and air saturation, measuring oxygen consumption by the Clark electrode [18].

In vivo ubiquitination

To evaluate whether hDASPO undergoes ubiquitination in the selected cell line, U87 3XFLAG-hDASPO_341 or -hDASPO_369 cells were transiently transfected with FLAG-ubiquitin and, 48 hours after transfection, the cells were treated for 6 hours with 25 μM MG132. Cells were subsequently collected by trypsinization, resuspended in denaturing lysis buffer (20 mM Tris-HCl, pH 8.0, 150 mM NaCl, 1% SDS and 1 mM EDTA, supplemented with **protease** inhibitors as above), boiled for 7 min and sonicated. The cell lysate was then centrifuged at 13000 g for 30 min at 4 °C and the supernatant was diluted 1:10 in IP buffer (20 mM Tris-HCl, pH 8.0, 150 mM NaCl, 0.5% NP-40, 0.5% Triton X-100 and 1 mM EDTA, supplemented with **protease** inhibitors). The FLAG-tagged hDASPO isoforms and ubiquitin where co-immunoprecipitated using ANTI-FLAG M2 Affinity Gel (Sigma). A volume of sample corresponding to 0.5 mg or 1 mg of total proteins for U87 3XFLAG-hDASPO_341 and -hDASPO_369 cells, respectively, was added to 50 μL of the ANTI-FLAG agarose resin and immunoprecipitation was performed as detailed above. The resin was resuspended in 50 μL of a non-reducing SDS-PAGE sample buffer (IP sample) and boiled. 20 μL of the IP samples were subjected to SDS-PAGE on an 8–15% polyacrylamide gel and the ubiquitin-hDASPO conjugates revealed by Western blot analysis using the anti-hDASPO antibody (Davids Biotechnologie).

HPLC analysis

To determine cellular D- and L-Asp levels, as well as D- and L-Ser, the cells stably expressing the 3XFLAG-hDASPO_341 variant were analyzed using the procedure reported in [15] with minor modifications. Cell pellets were homogenized in 1:5 (w/v) 0.2 M TCA, sonicated (three cycles, 10 s each) and the resulting cell extracts were clarified by centrifugation at 13,000 g for 20 min. The precipitated protein pellets were stored at −80 °C for quantification, while 10 μL of the supernatants were neutralized with NaOH and subjected to precolumn derivatization with 20 uL of 74.5 mM o-phthaldialdehyde (OPA) and 30.5 mM N-acetyl L-cysteine (NAC) in 50% methanol.

Diastereoisomer derivatives were resolved on a Symmetry C8 reversed-phase column (5 µm, 4.6 × 250 mm, Waters) under isocratic conditions (0.1 M sodium acetate buffer, pH 6.2, 1% tetrahydrofuran, and 1 mL/min flow rate). A washing step in 0.1 M sodium acetate buffer, 3% tetrahydrofuran, and 47% acetonitrile was performed after each run. Identification of peaks was based on retention times and confirmed by: i) adding known amounts of external standards to the samples, ii) by the selective degradation catalyzed by the M213R or wild-type RgDAAO for D-Asp and D-Ser, respectively: 10 µg of the enzymes were added to the samples, which were incubated at 30 °C for 60 min and then derivatized. The peak area for D-Asp or D-Ser corresponded to the one decreased following the enzymatic treatment. Total protein content of homogenates was determined using the Bradford assay method after resolubilization of the TCA precipitated protein pellets in 1% SDS. The total amount of D- and L-amino acids detected in cell extracts was normalized by the total protein content.

nLC-MS/MS analysis

To investigate the presence of hDASPO isoforms in hippocampal cortex from male and female healthy controls and AD patients, samples were analyzed by MS using a shotgun label free proteomic approach. Frozen hippocampus cortex samples were obtained from London Neurodegenerative Diseases Brain Bank (London, UK). Hippocampus tissues were homogenized using a Potter homogenizer in 200 µL of extraction buffer (8 M urea, 20 mM Hepes pH 8, with proteases and phosphatases inhibitors) at full speed for 1 min. The homogenate was sonicated 3 times for 20 ms on ice with a ultrasonic homogenizer and centrifuged at 13000 rpm for 15 min to sediment unhomogenized tissue and large cellular debris. The pellet was discarded and the protein content was determined by a Bradford assay (Sigma Aldrich). Proteins were subjected to reduction with 13 mM dithioerythritol (30 min at 55 °C) and alkylation with 26 mM iodoacetamide (IAA; 30 min at room temperature). Peptide digestion was conducted using sequence-grade trypsin (Promega) for 16 h at 37 °C using a protein: trypsin ratio of 20:1 [38]. The proteolytic digest was desalted using Zip-Tip C18

(Millipore) before MS analysis. LC-ESI-MS/MS analysis was performed on a on Dionex UltiMate 3000 directly connected to an Orbitrap Fusion Tribrid mass spectrometer (Thermo Fisher Scientific, Waltham, MA, USA) by a nanoelectrospray ion source. Peptide mixtures were enriched on 75 µm ID × 150 mm Acclaim PepMap RSLC C18 column and separated employing the following LC gradient: 4% ACN in 0.1% formic acid for 3 min, 4–28% ACN in 0.1% formic acid for 130 min, 28–40% ACN in 0.1% formic acid for 20 min, 40–95% ACN in 0.1% formic for 2 min and 95–4% ACN in 0.1% formic acid for 3 min at a flow rate of 0.3 µL/min. MS spectra of eluting peptides were collected over an m/z range of 375–1500 using a resolution setting of 120,000, operating in the data-dependent mode to automatically alternate between Orbitrap-MS and Orbitrap-MS/MS acquisition. HCD MS/MS spectra were collected for the 20 most abundant ions in each MS scan using a normalized collision energy of 30%, and an isolation window of 1.7 m/z. Rejection of +1, and unassigned charge states were enabled [39]. Raw label-free MS/MS files from Thermo Xcalibur software (version 4.1) [40] were analyzed using Proteome Discoverer software (version 1.4, Thermo Fisher Scientific) and searched with the Sequest algorithm against the hDASPO from Uniprot 05-11-2020. Only peptides with high confidence and a high cross correlation score (≥ 1.5) were considered. The minimum required peptide length was set to 6 amino acids with carbamidomethylation as fixed modification, Met oxidation and Arg/Gln deamidation as variable modifications.

Acknowledgements

This research was supported by Università degli studi dell'Insubria, grant "Fondo di Ateneo per la Ricerca" to SS and LP. VR is a Ph.D. student of the Biotechnology and Life Sciences course at the University of Insubria.

Conflict of interest

The authors declare no conflict of interest.

Author contributions

VR conceived, designed and performed the experiments under the supervision of SS. **GT and EM performed MS analysis,** LP conceived the work, contributed to the analysis and discussion of the results and critically revised the manuscript. All authors have read and agreed to the published version of the manuscript.

References

1. Still JL, Buell MV, Knox WE & Green DE (1949) Studies on the cyclophorase system; D-aspartic oxidase. *J Biol Chem* **179**, 831-837.

2. Takahashi S (2020) D-Aspartate oxidase: distribution, functions, properties, and biotechnological applications. *Appl Microbiol Biotechnol* **104**, 2883-2895.

3. Negri A, Massey V & Williams CH Jr (1987) D-aspartate oxidase from beef kidney. Purification and properties. *J Biol Chem* **262**, 10026-10034.

4. Pollegioni L, Piubelli L, Sacchi S, Pilone MS & Molla G (2007) Physiological functions of D-amino acid oxidases: from yeast to humans. *Cell Mol Life Sci* **64**, 1373-1394.

5. Di Fiore MM, Santillo A & Chieffi Baccari G (2014) Current knowledge of D-aspartate in glandular tissues. *Amino Acids* **46**, 1805-1818.

6. Dunlop DS, Neidle A, McHale D, Dunlop DM & Lajtha A (1986) The presence of free D-aspartic acid in rodents and man. *Biochem Biophys Res Commun* **141**, 27-32.

7. Hashimoto A, Kumashiro S, Nishikawa T, Oka T, Takahashi K, Mito T, Takashima S, Doi N, Mizutani Y, Yamazaki T, Kaneko T & Ootomo E (1993) Embryonic development and postnatal changes in free D-aspartate and D-serine in the human prefrontal cortex. *J Neurochem* **61**, 348-351.

8. Ota N, Shi T & Sweedler JV (2012) D-Aspartate acts as a signaling molecule in nervous and neuroendocrine systems. *Amino Acids* **43**, 1873-1886.

9. Cristino L, Luongo L, Squillace M, Paolone G, Mango D, Piccinin S, Zianni E, Imperatore R, Iannotta M, Longo F, Errico F, Vescovi AL, Morari M, Maione S, Gardoni F, Nisticò R & Usiello A (2015) D-Aspartate oxidase influences glutamatergic system homeostasis in mammalian brain. *Neurobiol Aging* **36**, 1890-1902.

10. Molinaro G, Pietracupa S, Di Menna L, Pescatori L, Usiello A, Battaglia G, Nicoletti F & Bruno V (2010) D-aspartate activates mGlu receptors coupled to polyphosphoinositide hydrolysis in neonate rat brain slices. *Neurosci Lett* **478**, 128-130.

11. Errico F, Nisticò R, Napolitano F, Mazzola C, Astone D, Pisapia T, Giustizieri M, D'Aniello A, Mercuri NB & Usiello A (2011) Increased D-aspartate brain content rescues hippocampal age-related synaptic plasticity deterioration of mice. *Neurobiol Aging* **32**, 2229-2243.

12. Schell MJ, Cooper OB & Snyder SH (1997) D-aspartate localizations imply neuronal and neuroendocrine roles. *Proc Natl Acad Sci U S A* **94**, 2013-2018.

13. Errico F, Napolitano F, Nisticò R, Centonze D & Usiello A (2009) D-aspartate: an atypical amino acid with neuromodulatory activity in mammals. *Rev Neurosci* **20**, 429-440.

14. Errico F, Napolitano F, Nisticò R & Usiello A (2012) New insights on the role of free D-aspartate in the mammalian brain. *Amino Acids* **43**, 1861-1871.

15. Punzo D, Errico F, Cristino L, Sacchi S, Keller S, Belardo C, Luongo L, Nuzzo T, Imperatore R, Florio E, De Novellis V, Affinito O, Migliarini S, Maddaloni G, Sisalli MJ, Pasqualetti M, Pollegioni L, Maione S, Chiariotti L & Usiello A (2016) Age-related changes in D-aspartate oxidase promoter methylation control extracellular D-aspartate levels and prevent precocious cell death during brain aging. *J Neurosci* **36**, 3064-3078.

16. Errico F, Nisticò R, Napolitano F, Oliva AB, Romano R, Barbieri F, Florio T, Russo C, Mercuri NB & Usiello A (2011) Persistent increase of D-aspartate in D-aspartate oxidase mutant mice induces a precocious hippocampal age-dependent synaptic plasticity and spatial memory decay. *Neurobiol Aging* **32**, 2061-2074.

17. Errico F, Nisticò R, Palma G, Federici M, Affuso A, Brilli E, Topo E, Centonze D, Bernardi G, Bozzi Y, D'Aniello A, Di Lauro R, Mercuri NB & Usiello A (2008) Increased levels of D-

aspartate in the hippocampus enhance LTP but do not facilitate cognitive flexibility. *Mol Cell Neurosci* **37**, 236-246.

18. Molla G, Chaves-Sanjuan A, Savinelli A, Nardini M & Pollegioni L (2020) Structure and kinetic properties of human D-aspartate oxidase, the enzyme-controlling D-aspartate levels in brain. *FASEB J* **34**, 1182-1197.

19. Setoyama C & Miura R (1997) Structural and functional characterization of the human brain D-aspartate oxidase. *J Biochem* **121**, 798-803.

20. Sacchi S, Novellis V, Paolone G, Nuzzo T, Iannotta M, Belardo C, Squillace M, Bolognesi P, Rosini E, Motta Z, Frassineti M, Bertolino A, Pollegioni L, Morari M, Maione S, Errico F & Usiello A (2017) Olanzapine, but not clozapine, increases glutamate release in the prefrontal cortex of freely moving mice by inhibiting D-aspartate oxidase activity. *Sci Rep* **7**, 46288.

21. Cappelletti P, Campomenosi P, Pollegioni L & Sacchi S (2014) The degradation (by distinct pathways) of human D-amino acid oxidase and its interacting partner pLG72--two key proteins in D-serine catabolism in the brain. *FEBS J* **281**, 708-723.

22. Zhao J, Zhai B, Gygi SP & Goldberg AL (2015) mTOR inhibition activates overall protein degradation by the ubiquitin proteasome system as well as by autophagy. *Proc Natl Acad Sci U S A* **112**, 15790-15797.

23. Ciechanover A (2005) Proteolysis: from the lysosome to ubiquitin and the proteasome. *Nat Rev Mol Cell Biol* **6**, 79-87.

24. Zhang T, Shen S, Qu J & Ghaemmaghami S (2016) Global Analysis of Cellular Protein Flux Quantifies the Selectivity of Basal Autophagy. *Cell Rep* **14**, 2426-2439.

25. Amenta JS, Hlivko TJ, McBee AG, Shinozuka H & Brocher S (1978) Specific inhibition by NH4CL of autophagy-associated proteloysis in cultured fibroblasts. *Exp Cell Res* **115**, 357-366.

26. Mauthe M, Orhon I, Rocchi C, Zhou X, Luhr M, Hijlkema KJ, Coppes RP, Engedal N, Mari M & Reggiori F (2018) Chloroquine inhibits autophagic flux by decreasing autophagosome-lysosome fusion. *Autophagy* **14**, 1435-1455.

27. Groll M & Huber R (2004) Inhibitors of the eukaryotic 20S proteasome core particle: a structural approach. *Biochim Biophys Acta* **1695**, 33-44.

28. Le Bail M, Martineau M, Sacchi S, Yatsenko N, Radzishevsky I, Conrod S, Ait Ouares K, Wolosker H, Pollegioni L, Billard JM & Mothet JP (2015) Identity of the NMDA receptor coagonist is synapse specific and developmentally regulated in the hippocampus. *Proc Natl Acad Sci U S A* **112**, E204-E213.

29. Pollegioni L & Sacchi S (2010) Metabolism of the neuromodulator D-serine. *Cell Mol Life Sci* **67**, 2387-2404.

30. Wolosker H (2011) Serine racemase and the serine shuttle between neurons and astrocytes. *Biochim Biophys Acta* **1814**, 1558-1566.

31. Sacchi S, Caldinelli L, Cappelletti P, Pollegioni L & Molla G (2012) Structure-function relationships in human D-amino acid oxidase. *Amino Acids* **43**, 1833-1850.

32. Mellman WJ, Schimke RT & Hayflick L (1972) Catalase turnover in human diploid cell cultures. *Exp Cell Res* **73**, 399-409.

33. Huybrechts SJ, Van Veldhoven PP, Brees C, Mannaerts GP, Los GV & Fransen M (2009) Peroxisome dynamics in cultured mammalian cells. *Traffic* **10**, 1722-1733.

34. Nordgren M, Wang B, Apanasets O & Fransen M (2013) Peroxisome degradation in mammals: mechanisms of action, recent advances, and perspectives. *Front Physiol* **4**, 145.

35. Léon S, Goodman JM & Subramani S (2006) Uniqueness of the mechanism of protein import into the peroxisome matrix: transport of folded, co-factor-bound and oligomeric proteins by shuttling receptors. *Biochim Biophys Acta* **1763**, 1552-1564.

36. Leithe E & Rivedal E (2004) Epidermal growth factor regulates ubiquitination, internalization and proteasome-dependent degradation of connexin43. *J Cell Sci* **117**, 1211-1220.

37. Katane M, Yamada S, Kawaguchi G, Chinen M, Matsumura M, Ando T, Doi I, Nakayama K, Kaneko Y, Matsuda S, Saitoh Y, Miyamoto T, Sekine M, Yamaotsu N, Hirono S & Homma H (2015) Identification of novel D-Aspartate oxidase inhibitors by in silico screening and their functional and structural characterization in vitro. *J Med Chem* **58**, 7328-7340.

38. Eberini I, Calabresi L, Wait R, Tedeschi G, Pirillo A, Puglisi L & Sirtori C (2002) Macrophage metalloproteinases degrade high-density-lipoprotein-associated apolipoprotein A-1 at both the N- and C- terminal. *Biochem J* 362, 627-634.

39. Tamplenizza M, Lenardi C, Maffioli E, Nonnis S, Negri A, Forti S, Sogne E, De Astis S, Matteoli M, Schulte C, Milani P & Tedeschi G (2013) Nitric oxide synthase mediates PC12 differentiation induced by the surface topography of nanostructured TiO2. *J Nanobiotec* 35, 1477-3155.

40. Tedeschi G, Albani E, Borroni EM, Parini V, Brucculeri AM, Maffioli E, Negri A, Nonnis S, Maccarrone M & Levi-Setti PE (2017) Proteomic profile of maternal-aged blastocoel fluid suggests a novel role for ubiquitin system in blastocyst quality *J Assist Reprod Genet* 34(2), 225-238.

Figures legends:

Fig. 1: Expression of hDASPO isoforms in U87 glioblastoma cells. (A, B) Relative expression levels of the protein isoforms in U87 cell clones stably transfected with pcDNA3 3XFLAG-hDASPO_341 (clones 27 and 38) or pcDNA3 3XFLAG-hDASPO_369 (clones 15 and 30) detected by Western blot analysis using anti-hDASPO antibody (A) and corresponding densitometric analysis (panel B; grey bars: hDASPO_341; white bars: hDASPO_369). Amounts of sample corresponding to 5×10^4 cells were loaded. $Ctrl^-$ represents the untrasfected cells sample and recombinant hDASPO (38.6 kDa) was used as a positive control. (C, D) IP studies aimed to confirm the identity of the hDASPO forms detected in lysates of U87 cells transfected with pcDNA3 3XFLAG-hDASPO_369. The presence of hDASPO was revealed by Western blot analysis using anti-hDASPO antibody: (C) 3XFLAG-hDASPO_369 (44 kDa) was immunoprecipitated from the whole cell lysate using an anti-FLAG agarose resin and (D) the ensuing post-IP sample (showing bands at 37 and 40.5 kDa) was further immunoprecipitated using anti-hDASPO antibodies conjugated to Dynabeads Protein G. Bands corresponding to 3XFLAG-hDASPO_369 (44 kDa) and hDASPO_341 (40.5 kDa) were observed in the IP I and IP II samples, respectively.

Fig. 2: HPLC analysis of the cellular content of Asp and Ser enantiomers. The amount of D- and L-Asp (A) and of D- and L-Ser (B) in U87 cells stably transfected with pcDNA3_3xFLAG-hDASPO_341 and in control cells transfected with the empty vector, was measured and normalized for the total protein content in each sample. The D-enantiomer/total stereoisomers ratio is also reported (right panels). ***$p < 0.0001$. Data were analyzed by unpaired parametric t-test. Graphs report single data point as well as mean values.

Fig. 3: Confocal analysis of U87 stable clones expressing 3XFLAG-hDASPO protein isoforms and control cells. U87 untransfected cells, as well as 3XFLAG-hDASPO_369 (B, E) and 3XFLAG-hDASPO_341 (C, F) expressing cells were double-stained with the anti-FLAG and the anti-PMP70

(A-C) or the anti-hDASPO and the anti-mitochondria antibodies (D-F). (A, D) Control cells showed no (aspecific) signals either with the red (A) or the green (D) channel, respectively. (B, C) 3XFLAG-hDASPO_369 (B) and 3XFLAG-hDASPO_341 (C) signals (red channel) largely overlapped with PMP70 ones (green channel), strongly indicating a peroxisomal localization for both protein isoforms. (E, F) No signal overlapping with the **signal for** mitochondria is instead observed for both the 3XFLAG-hDASPO_369 (E) and _341 (F) hDASPO isoforms (compare the signal distribution in the merge panels). Scale bars: 10 µm.

Fig. 4: Analysis of hDASPO degradation rate. U87 cells stably expressing 3XFLAG-hDASPO_369 or 3XFLAG-hDASPO_341 isoforms were treated with 100 µg/mL CHX. (A) In U87 3XFLAG-hDASPO_369 CHX-treated cells, only a small decrease (~20% at 32 h) in the signal detected at 39 kDa (untagged hDASPO_341) and 44 kDa (3XFLAG-hDASPO_369) by anti-hDASPO antibodies was apparent compared to the control. (B) Similarly, a small change in the intensity of the 42 kDa band corresponding to 3XFLAG-hDASPO_341 was observed following CHX addition, thus indicating that both the protein isoforms are highly stable. Values are the mean ± SD (n = 4-8), normalized to tubulin and expressed relatively to the control without CHX (i.e. cells collected at the same time after the addition of PBS).

Fig. 5: Effect of inhibitors of the degradation pathways on 3XFLAG-hDASPO_369 and 3XFLAG-hDASPO_341 cellular levels. (A) The cell clones were incubated under starvation conditions and treated with 75 µM CQ or PBS as a control, for up to 10 h. Western blot and quantification analysis showed no variation in the amount of 3XFLAG-hDASPO_369 (white bars) or 3XFLAG-hDASPO_341 (grey bars) in treated cells compared to controls. (B) U87 cells stably expressing 3XFLAG-hDASPO_369 or 3XFLAG-hDASPO_341 under starvation were treated with 25 µM MG132 or 0.1% DMSO for up to 10 h. Western blot analysis using anti-hDASPO antibody and quantitative analysis demonstrated that both 3XFLAG-hDASPO_369 and 3XFLAG-hDASPO_341

significantly accumulated after adding the inhibitor. For each time point, the value is expressed as the mean ± SD (n = 4), normalized to tubulin, and expressed relative to the control (i.e. cells collected at the same time after adding PBS or DMSO, see left lanes in Western blot panels).

Fig. 6: *In vitro* ubiquitination assay of recombinant hDASPO. The purified recombinant hDASPO (5 µg) was incubated with U87 cell extracts (4 mg/mL), ubiquitin, ATP, MG132 and ubiquitin aldehyde (in a final volume of 60 µL) and incubated at 37 °C for 60 minutes. To detect the formation of hDASPO-ubiquitin conjugates, an aliquot of the reaction mixture (corresponding to 0.625 µg of recombinant protein) was analyzed by Western blotting using anti-hDASPO antibody. (A) Distinct bands, corresponding to distinct hDASPO modified forms (mono- or polyubiquitinated) were evident in the reaction mixture only (lane 3) and absent in control samples (prepared by omitting ubiquitin, lane 2, or using the same volume of the reaction mixture without adding the recombinant protein, lane 1). The arrow indicates the unmodified protein. (B) Activity assays performed on the in vitro ubiquitination and control mixtures revealed that recombinant hDASPO activity is not affected by the modification. Activity measurements are reported as relative activity after the incubation at 37 °C compared to the starting value. Data represent mean values ± standard deviation (n=3).

Fig. 7: Ubiquitination analysis in U87 cells stably expressing hDASPO isoforms and transiently transfected with FLAG-ubiquitin. Forty-eight hours after transfection with pCMV-FLAG-ubiquitin, U87 control cells (lane 7) and cells stably expressing the 3XFLAG-hDASPO_369 (lanes 1-3) and -hDASPO_341 (lanes 4-6) isoforms were treated with 25 µM MG132 for 6 hours and then proteins were immunoprecipitated under denaturing conditions using anti-FLAG M2 Affinity resin. Cells transfected but not treated with the proteasome inhibitor or not transfected and added with MG132 were processed as controls. Dashed lines represent non continuous lanes. The presence of ubiquitinated-hDASPO was revealed by Western blot analysis using anti-hDASPO antibody.

Table 1. List of the hDASPO peptides identified by mass spectrometry in hippocampus samples from male and female healthy controls and Alzheimer's disease (AD) patients. The N-terminal peptide present in the hDASPO_369 isoform is marked in bold.

	Control		AD	
Sequence	**Male**	**Female**	**Male**	**Female**
1-**MRPARHWETR**-10	-	-	-	X
147-**MTEAELKKFPQYVFGQAFTTLK**-168	X	-	-	X
155-**FPQYVFGQAFTTLK**-168	-	-	X	-
184-**GSGGWTLTR**-192	X	X	-	X
194-**IEDLWELHPSFDIVVNCSGLGSR**-216	-	X	-	-
266-**QKGDWNLSPDAENSR**-280	X	-	-	-
266-**QKGDWNLSPDAENSREILSR**-285	X	-	X	X
268-**GDWNLSPDAENSREILSRCCALEPSLHGACNIR**300	-	-	-	X
268-**GDWNLSPDAENSREILSR**-280	-	X	-	-
314-**LQTELLAR**-321	X	-	-	-

Fig. 1

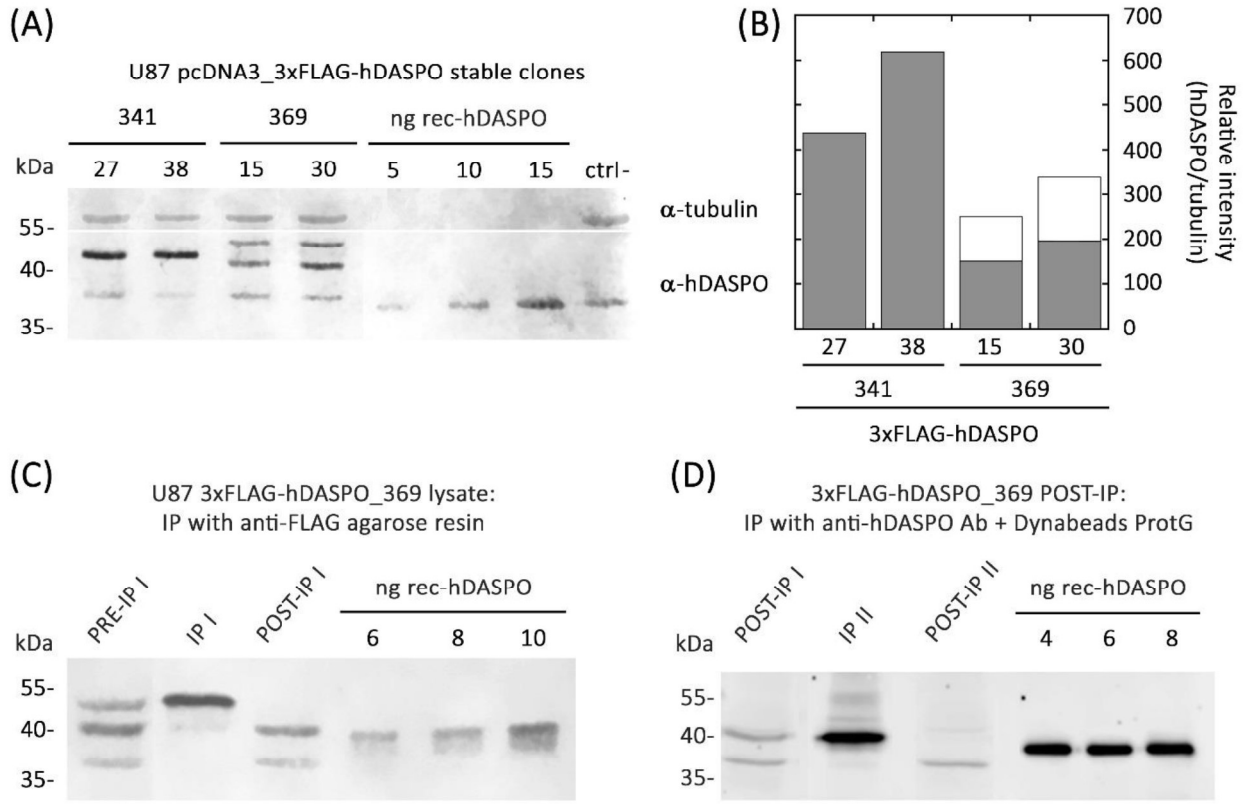
(A)
U87 pcDNA3_3xFLAG-hDASPO stable clones
341
369
ng rec-hDASPO
kDa
27
38
15
30
5
10
15
ctrl-
55-
40-
35-
α-tubulin
α-hDASPO
(B)
Relative intensity (hDASPO/tubulin)
700
600
500
400
300
200
100
0
27
38
15
30
341
369
3xFLAG-hDASPO
(C)
U87 3xFLAG-hDASPO_369 lysate:
IP with anti-FLAG agarose resin
PRE-IP I
IP I
POST-IP I
ng rec-hDASPO
6
8
10
kDa
55-
40-
35-
(D)
3xFLAG-hDASPO_369 POST-IP:
IP with anti-hDASPO Ab + Dynabeads ProtG
POST-IP I
IP II
POST-IP II
ng rec-hDASPO
4
6
8
kDa
55-
40-
35-

Fig. 2

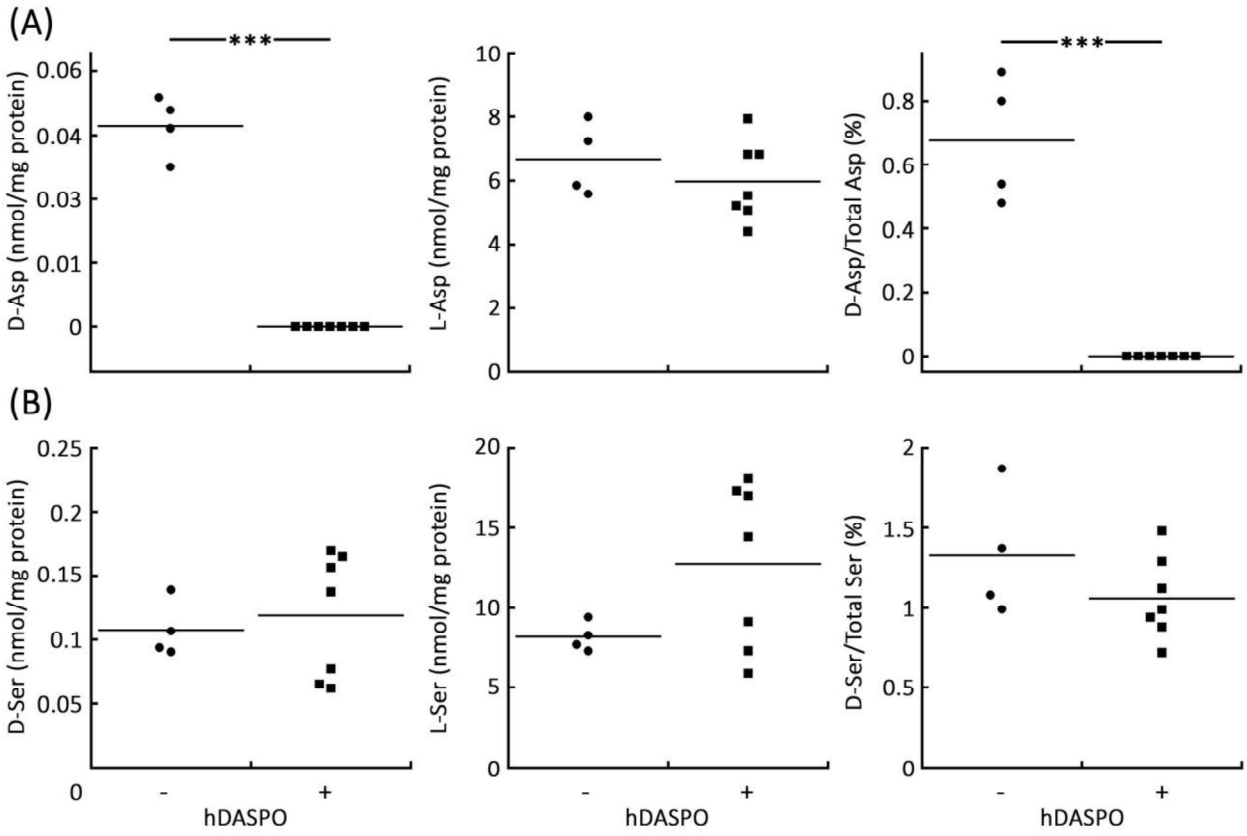
(A)
***
D-Asp (nmol/mg protein)
0.06
0.04
0.03
0.01
0
L-Asp (nmol/mg protein)
10
8
6
4
2
0
***
D-Asp/Total Asp (%)
0.8
0.6
0.4
0.2
0
(B)
D-Ser (nmol/mg protein)
0.25
0.2
0.15
0.1
0.05
0
-
+
hDASPO
L-Ser (nmol/mg protein)
20
15
10
5
0
-
+
hDASPO
D-Ser/Total Ser (%)
2
1.5
1
0.5
0
-
+
hDASPO

Fig. 3

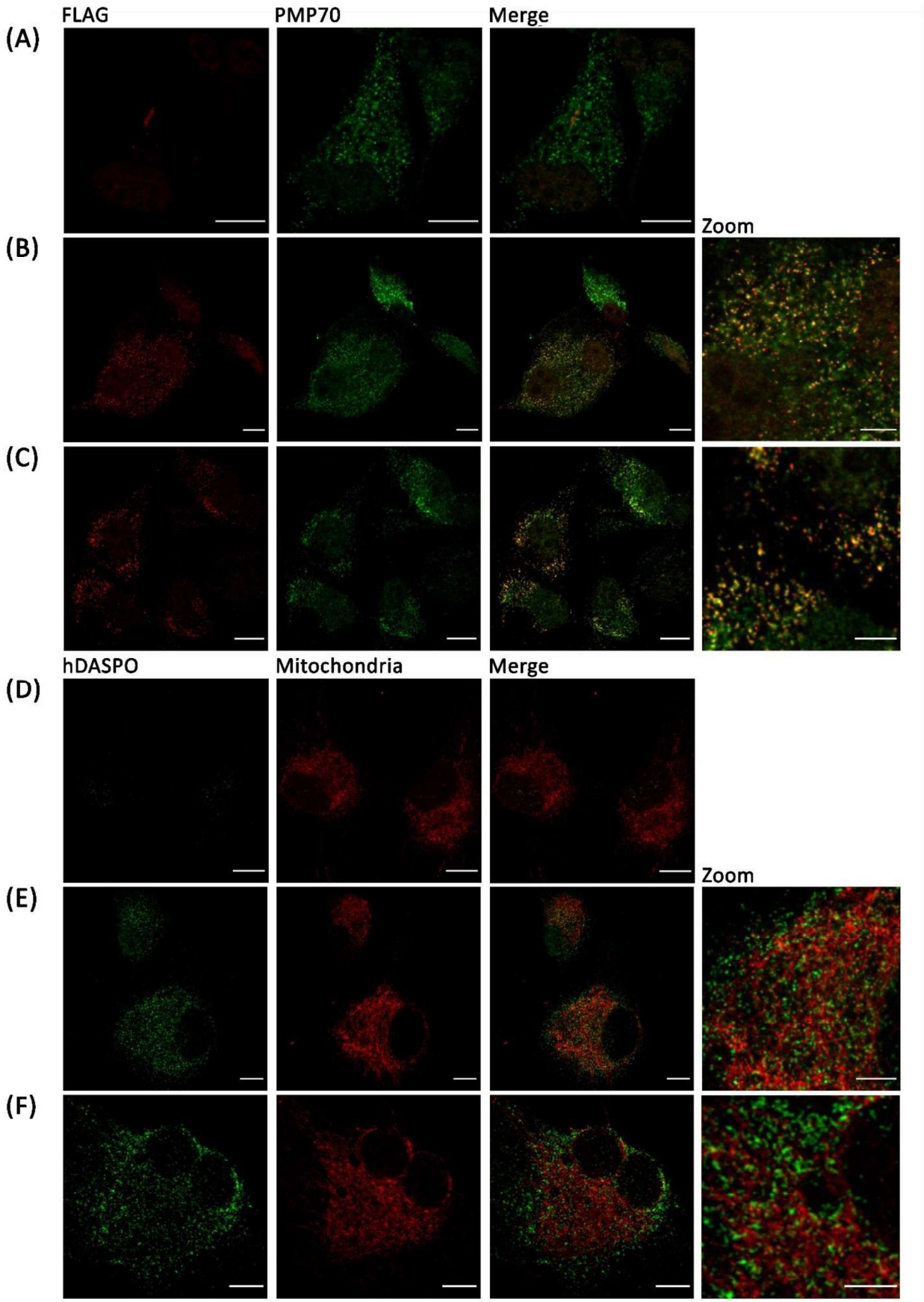
FLAG
PMP70
Merge
(A)
Zoom
(B)
(C)
hDASPO
Mitochondria
Merge
(D)
Zoom
(E)
(F)

Fig. 4

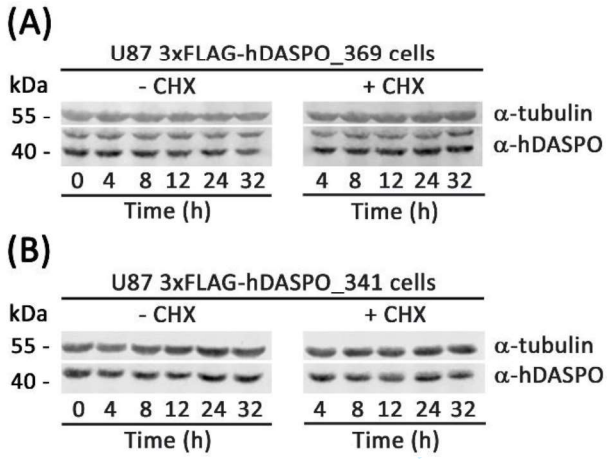
(A)
U87 3xFLAG-hDASPO_369 cells
kDa
- CHX
+ CHX
55 -
40 -
α-tubulin
α-hDASPO
0 4 8 12 24 32
4 8 12 24 32
Time (h)
Time (h)
(B)
U87 3xFLAG-hDASPO_341 cells
kDa
- CHX
+ CHX
55 -
40 -
α-tubulin
α-hDASPO
0 4 8 12 24 32
4 8 12 24 32
Time (h)
Time (h)

Fig. 5

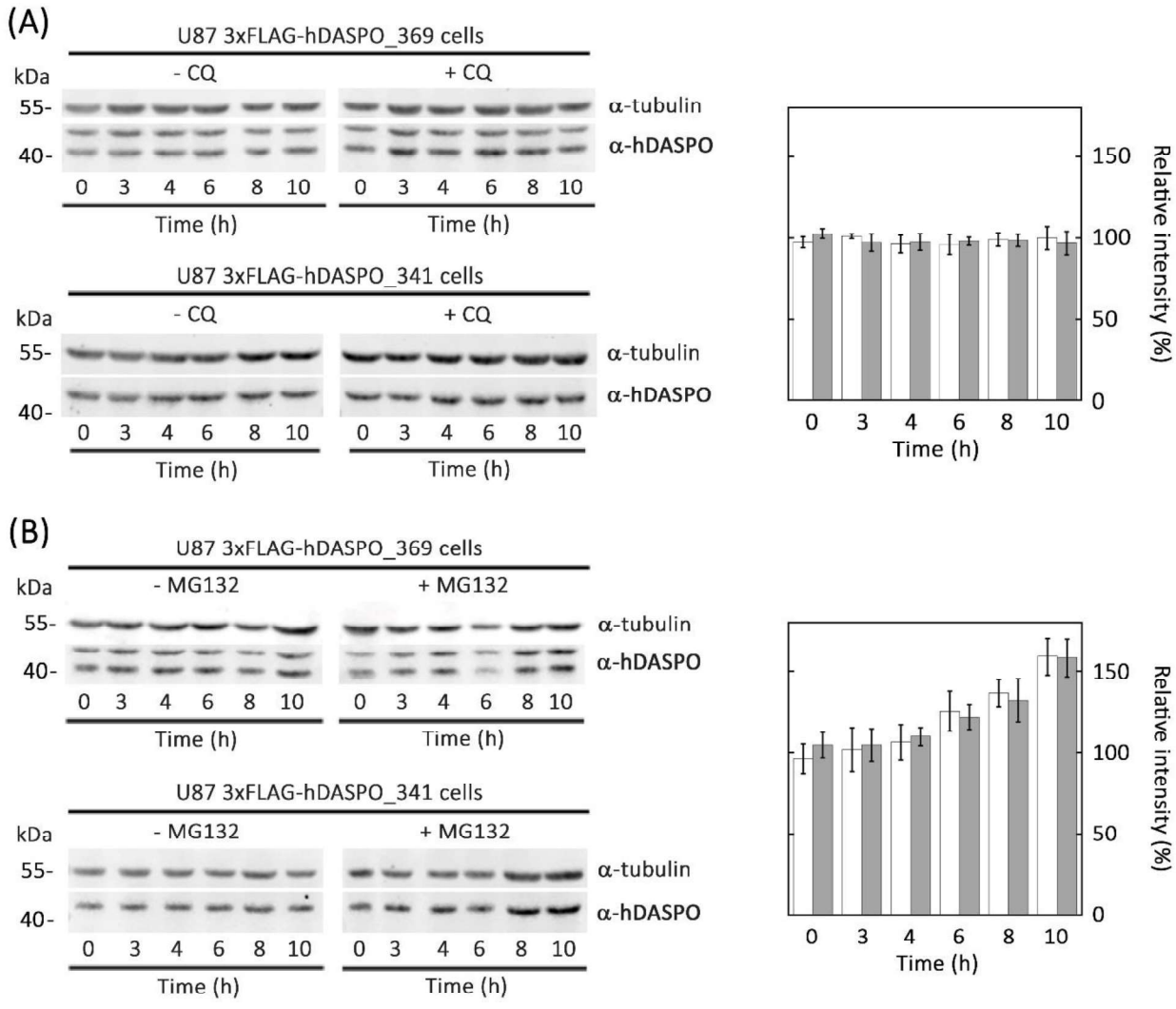
(A)
U87 3xFLAG-hDASPO_369 cells
kDa
- CQ
+ CQ
55-
40-
α-tubulin
α-hDASPO
0 3 4 6 8 10
0 3 4 6 8 10
Time (h)
Time (h)
U87 3xFLAG-hDASPO_341 cells
kDa
- CQ
+ CQ
55-
40-
α-tubulin
α-hDASPO
0 3 4 6 8 10
0 3 4 6 8 10
Time (h)
Time (h)
(B)
U87 3xFLAG-hDASPO_369 cells
kDa
- MG132
+ MG132
55-
40-
α-tubulin
α-hDASPO
0 3 4 6 8 10
0 3 4 6 8 10
Time (h)
Time (h)
U87 3xFLAG-hDASPO_341 cells
kDa
- MG132
+ MG132
55-
40-
α-tubulin
α-hDASPO
0 3 4 6 8 10
0 3 4 6 8 10
Time (h)
Time (h)
150
100
50
0
Relative intensity (%)
0 3 4 6 8 10
Time (h)
150
100
50
0
Relative intensity (%)
0 3 4 6 8 10
Time (h)

Fig. 6

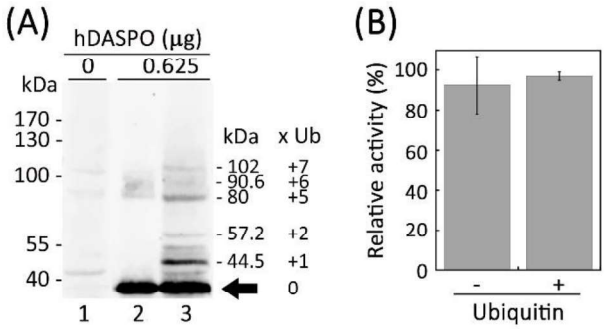

Fig. 7

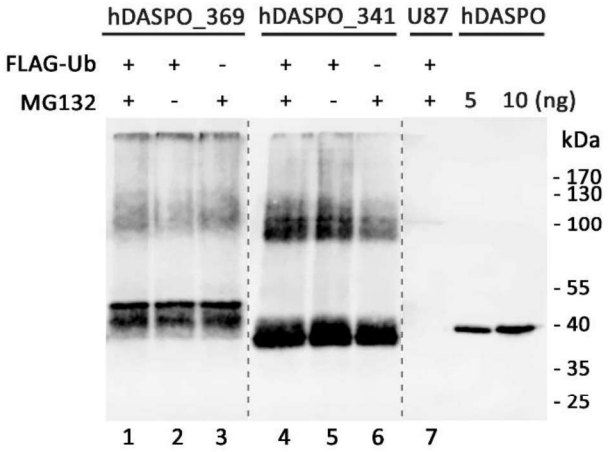

Supporting Information:

Supplementary Table 1. **Conditions used to solubilize recombinant hDASPO_369 from *E. coli* inclusion bodies.**

Supplementary Table 2. **Bioinformatics prediction of protein solubility for hDASPO isoforms.**

Supplementary Table ***3***. Primers used for cloning human hDASPO_341 and hDASPO_369 cDNA in the pcDNA3 mammalian expression vector.

Supplementary Figure 1. **Multiple sequence alignment of hDASPO isoforms.**

Supplementary Figure 1. **Multiple sequence alignment of hDASPO isoforms using ClustalW. Peptide sequences identified in hippocampus samples from healthy controls and Alzheimer's disease patients are highlighted in light grey. N-terminal peptide present in the 369 isoform, identified solely in hippocampus of female AD patients, is highlighted in dark grey.**

```
SP|Q99489|OXDD_HUMAN   ----------------------------MDTARIAVVGAGVVGLSTAVCISKLVPRCSVT 32
SP|Q99489-2|OXDD_HUMAN ----------------------------MDTARIAVVGAGVVGLSTAVCISKLVPRCSVT 32
SP|Q99489-3|OXDD_HUMAN MRPARHWETRFGARDFGGFQDCFFRDRLMDTARIAVVGAGVVGLSTAVCISKLVPRCSVT 60
                                                    ********************************

SP|Q99489|OXDD_HUMAN   IISDKFTPDTTSDVAAGMLIPHTYPDTPIHTQKQWFRETFNHLFAIANSAEAGDAGVHLV 92
SP|Q99489-2|OXDD_HUMAN IISDKFTPDTTSDVAAGMLIPHTYPDTPIHTQKQWFRETFNHLFAIANSAEAGDAGVHLV 92
SP|Q99489-3|OXDD_HUMAN IISDKFTPDTTSDVAAGMLIPHTYPDTPIHTQKQWFRETFNHLFAIANSAEAGDAGVHLV 120
                        ************************************************************

SP|Q99489|OXDD_HUMAN   SGWQIFQSTPTEEVPFWADVVLGFRKMTEAELKKFPQYVFGQAFTTLKCECPAYLPWLEK 152
SP|Q99489-2|OXDD_HUMAN SG------------------------------------------------------- 94
SP|Q99489-3|OXDD_HUMAN SGWQIFQSTPTEEVPFWADVVLGFRKMTEAELKKFPQYVFGQAFTTLKCECPAYLPWLEK 180
                        **

SP|Q99489|OXDD_HUMAN   RIKGSGGWTLTRRIEDLWELHPSFDIVVNCSGLGSRQLAGDSKIFPVRGQVLQVQAPWVE 212
SP|Q99489-2|OXDD_HUMAN -IKGSGGWTLTRRIEDLWELHPSFDIVVNCSGLGSRQLAGDSKIFPVRGQVLQVQAPWVE 153
SP|Q99489-3|OXDD_HUMAN RIKGSGGWTLTRRIEDLWELHPSFDIVVNCSGLGSRQLAGDSKIFPVRGQVLQVQAPWVE 240
                         ************************************************************

SP|Q99489|OXDD_HUMAN   HFIRDGSGLTYIYPGTSHVTLGGTRQKGDWNLSPDAENSREILSRCCALEPSLHGACNIR 272
SP|Q99489-2|OXDD_HUMAN HFIRDGSGLTYIYPGTSHVTLGGTRQKGDWNLSPDAENSREILSRCCALEPSLHGACNIR 213
SP|Q99489-3|OXDD_HUMAN HFIRDGSGLTYIYPGTSHVTLGGTRQKGDWNLSPDAENSREILSRCCALEPSLHGACNIR 300
                        ************************************************************

SP|Q99489|OXDD_HUMAN   EKVGLRPYRPGVRLQTELLARDGQRLPVVHHYGHGSGGISVHWGTALEAARLVSECVHAL 332
SP|Q99489-2|OXDD_HUMAN EKVGLRPYRPGVRLQTELLARDGQRLPVVHHYGHGSGGISVHWGTALEAARLVSECVHAL 273
SP|Q99489-3|OXDD_HUMAN EKVGLRPYRPGVRLQTELLARDGQRLPVVHHYGHGSGGISVHWGTALEAARLVSECVHAL 360
                        ************************************************************

SP|Q99489|OXDD_HUMAN   RTPIPKSNL 341
SP|Q99489-2|OXDD_HUMAN RTPIPKSNL 282
SP|Q99489-3|OXDD_HUMAN RTPIPKSNL 369
                        *********
```

Supplementary Table 1. **Procedures and conditions for hDASPO_369 inclusion bodies solubilization and refolding.**

Column-based procedure:

Conditions	1	2	3	4
IB solubilization	Solubilization buffer	Solubilization buffer	Solubilization buffer + 10 µM FAD	Solubilization buffer
Column wash	Wash buffer (20 mM imidazole)	Wash buffer (5 mM imidazole)	Wash buffer (5 mM imidazole) + 10 µM FAD	
Refolding	Refolding buffer (20 mM imidazole)	Refolding buffer (5 mM imidazole)	Refolding buffer (5 mM imidazole)	Refolding buffer (5 mM imidazole)
Elution	Elution buffer	Elution buffer	Elution buffer	Elution buffer

Dialysis-based procedure:

Conditions	1	2	3
IB solubilization	Solubilization buffer (1 mM 2-mercaptoethanol) + 40 µM FAD	Solubilization buffer (5 mM 2-mercaptoethanol) + 40 µM FAD	50 mM Tris-HCl pH 8.0, 2 M urea, 6 M *n*-propanol, 40 µM FAD
buffer 1	20 mM Tris–HCl pH 8.0, 4 M guanidine hydrochloride, 0.5 M NaCl, 5 mM Na/K tartrate, 1 mM 2-mercaptoethanol, 40 µM FAD	20 mM Tris–HCl pH 8.0, 4 M guanidine hydrochloride, 0.5 M NaCl, 5 mM Na/K tartrate, 5 mM 2-mercaptoethanol, 40 µM FAD	20 mM Tris–HCl pH 8.0, 2 M urea, 4 M *n*-propanol, 0.25 M NaCl, 5 mM Na/K tartrate, 1 mM 2-mercaptoethanol, 40 µM FAD
buffer 2	20 mM Tris–HCl pH 8.0, 2 M guanidine hydrochloride, 0.25 M NaCl, 5 mM Na/K tartrate, 1 mM 2-mercaptoethanol, 40 µM FAD	20 mM Tris–HCl pH 8.0, 2 M guanidine hydrochloride, 0.25 M NaCl, 5 mM Na/K tartrate, 5 mM 2-mercaptoethanol, 40 µM FAD	20 mM Tris–HCl pH 8.0, 2 M urea, 2 M *n*-propanol, 0.25 M NaCl, 5 mM Na/K tartrate, 1 mM 2-mercaptoethanol, 40 µM FAD
buffer 3	20 mM Tris–HCl pH 8.0, 1 M guanidine hydrochloride, 0.1 M NaCl, 5 mM Na/K tartrate, 1 mM 2-mercaptoethanol, 40 µM FAD	20 mM Tris–HCl pH 8.0, 1 M guanidine hydrochloride, 0.1 M NaCl, 5 mM Na/K tartrate, 200 mM arginine, 350 µM oxidized glutathione, 5 mM 2-mercaptoethanol, 40 µM FAD	20 mM Tris–HCl pH 8.0, 2 M urea, 0.25 M NaCl, 5 mM Na/K tartrate, 1 mM 2-mercaptoethanol, 40 µM FAD

buffer 4	**20 mM Tris–HCl pH 8.0, 0.5 M guanidine hydrochloride, 0.1 M NaCl, 5 mM Na/K tartrate, 1 mM 2-mercaptoethanol, 40 µM FAD**	**20 mM Tris–HCl pH 8.0, 0.5 M guanidine hydrochloride, 0.1 M NaCl, 5 mM Na/K tartrate, 200 mM arginine, 350 µM oxidized glutathione, 5 mM 2-mercaptoethanol, 40 µM FAD**	**20 mM Tris–HCl pH 8.0, 1 M urea, 0.25 M NaCl, 5 mM Na/K tartrate, 1 mM 2-mercaptoethanol, 40 µM FAD**
buffer 5	**20 mM Tris–HCl pH 8.0, 0.1 M NaCl, 5 mM Na/K tartrate, 5% glycerol, 1 mM 2-mercaptoethanol, 40 µM FAD**	**20 mM Tris–HCl pH 8.0, 0.1 M NaCl, 5 mM Na/K tartrate, 5% glycerol, 5 mM 2-mercaptoethanol, 40 µM FAD**	**20 mM Tris–HCl pH 8.0, 0.25 M NaCl, 5 mM Na/K tartrate, 5% glycerol, 1 mM 2-mercaptoethanol, 40 µM FAD**
buffer 6	**20 mM Tris–HCl pH 8.0, 0.1 M NaCl, 10% glycerol, 1 mM 2-mercaptoethanol, 10 µM FAD**	**20 mM Tris–HCl pH 8.0, 0.1 M NaCl, 10% glycerol, 5 mM 2-mercaptoethanol, 10 µM FAD**	**20 mM Tris–HCl pH 8.0, 0.1 M NaCl, 10% glycerol, 1 mM 2-mercaptoethanol, 10 µM FAD**

Solubilization buffer: 20 mM Tris-HCl pH 8.0, 6 M guanidine hydrochloride, 0.5 M NaCl, 5 mM imidazole, 1 mM 2-mercaptoethanol.
Wash buffer: 20 mM Tris-HCl pH 8.0, 6 M urea, 0.5 M NaCl, 20 mM imidazole, 1 mM 2-mercaptoethanol. Refolding buffer: 20 mM Tris-HCl pH 8.0, 0.5 M NaCl, 20 mM imidazole, 1 mM 2-mercaptoethanol, 40 µM FAD.
Elution buffer: 20 mM Tris–HCl pH 8.0, 0.5 M NaCl, 500 mM imidazole, 1 mM 2-mercaptoethanol, 40 µM FAD.
For the column-based procedure, inclusion bodies derived from 500 mL of starting culture were resuspended in 20 mL of solubilization buffer; while for the dialysis-based procedure inclusion bodies derived from 150 mL of starting culture were resuspended in 10 mL of solubilization buffer. In the latter case, after solubilization the protein was dialyzed at 4 °C, in 500 mL of the indicated buffers, for 90 min (buffers 1-5) and overnight (buffer 6).

Supplementary Table 2. **Bioinformatics prediction of protein solubility for hDASPO isoforms.**

Software	Value	Score		Website	Reference
		hDASPO_341	hDASPO_369		
Protein-sol	Predicted scaled solubility	0.208	0.163	https://protein-sol.manchester.ac.uk/	Hebditch M, Carballo-Amador MA, Charonis S, Curtis R, Warwicker J. Protein-Sol: a web tool for predicting protein solubility from sequence. *Bioinformatics*. 2017;33(19):3098-3100. doi:10.1093/bioinformatics/btx345
Recombinant protein solubility prediction	Chance of solubility when overexpressed in *E. coli*	97.9%	0.0%	http://www.biotech.ou.edu/	Diaz AA, Tomba E, Lennarson R, Richard R, Bagajewicz MJ, Harrison RG. Prediction of protein solubility in Escherichia coli using logistic regression. *Biotechnol Bioeng*. 2010;105(2):374-383. doi:10.1002/bit.22537
Scratch (SOLpro)	Predicted solubility upon overexpression (probability)	0.910402	0.661469	http://scratch.proteomics.ics.uci.edu/	Magnan CN, Randall A, Baldi P. SOLpro: accurate sequence-based prediction of protein solubility. *Bioinformatics*. 2009;25(17):2200-2207. doi:10.1093/bioinformatics/btp386
SoluProt	Solubility	0.319	0.265	https://loschmidt.chemi.muni.cz/solup	Hon, J., Marusiak, M., Martinek, T., Zendulka J., Bednar, D., Damborsky, J., (2020) SoluProt: prediction of soluble expression from protein sequence. *Bioinformatics* (in preparation)

Supplementary Table 3. Primers used for cloning human hDASPO_341 and hDASPO_369 cDNA in the pcDNA3 mammalian expression vector **and in the pET11a prokaryotic expression vector**. Sequences recognized by the indicated endonucleases are underlined. In bold is reported the sequence encoding for the 3XFLAG peptide.

Oligo	**Sequence**	**Cloning site**
3XFLAG hDASPO 341_for	5'-ACAGCGGGATCCCACC**ATGGATTACAAGGATGACGACGATAAGGACTATAAGGACGATGATGACAAGGACTACAAAGATGATGACGATAAAC**TCGACACAGCACGGATTGCAGTTGTCG-3'	BamHI
3XFLAG hDASPO 369_for	5'-ACAGCGGGTACCCACC**ATGGATTACAAGGATGACGACGATAAGGACTATAAGGACGATGATGACAAGGACTACAAAGATGATGACGATAAAC**TCAGACCAGCCAGGCACTGGGAAACAAG-3'	KpnI
3XFLAG hDASPO 341/369_rev	5'-ACAGCGGCGGCCGCCTACAGGTTTGACTTGGGAATGGGGG-3'	NotI
pET11_hDASPO**369_for**	**5'-GTCTACATATGCACCATCACCATCATCACATGC-3'**	**NdeI**
pET11_hDASPO369_rev	**5'-CTGTTGGATCCTCATTACAGGTTTGATTTGGGAATCG-3'**	**BamHI**

Supporting information

Supplementary Figure 1. Multiple sequence alignment of hDASPO isoforms using ClustalW. Peptide sequences identified in hippocampus samples from healthy controls and Alzheimer's disease patients are highlighted in light grey. N-terminal peptide present in the 369 isoform, identified solely in hippocampus of female AD patients, is highlighted in dark grey.

```
SP|Q99489|OXDD_HUMAN   ----------------------------MDTARIAVVGAGVVGLSTAVCISKLVPRCSVT 32
SP|Q99489-2|OXDD_HUMAN ----------------------------MDTARIAVVGAGVVGLSTAVCISKLVPRCSVT 32
SP|Q99489-3|OXDD_HUMAN MRPARHWETRFGARDFGGFQDCFFRDRLMDTARIAVVGAGVVGLSTAVCISKLVPRCSVT 60
                                                    **********************************

SP|Q99489|OXDD_HUMAN   IISDKFTPDTTSDVAAGMLIPHTYPDTPIHTQKQWFRETFNHLFAIANSAEAGDAGVHLV 92
SP|Q99489-2|OXDD_HUMAN IISDKFTPDTTSDVAAGMLIPHTYPDTPIHTQKQWFRETFNHLFAIANSAEAGDAGVHLV 92
SP|Q99489-3|OXDD_HUMAN IISDKFTPDTTSDVAAGMLIPHTYPDTPIHTQKQWFRETFNHLFAIANSAEAGDAGVHLV 120
                        ************************************************************

SP|Q99489|OXDD_HUMAN   SGWQIFQSTPTEEVPFWADVVLGFRKMTEAELKKFPQYVFGQAFTTLKCECPAYLPWLEK 152
SP|Q99489-2|OXDD_HUMAN SG------------------------------------------------------- 94
SP|Q99489-3|OXDD_HUMAN SGWQIFQSTPTEEVPFWADVVLGFRKMTEAELKKFPQYVFGQAFTTLKCECPAYLPWLEK 180
                        **

SP|Q99489|OXDD_HUMAN   RIKGSGGWTLTRRIEDLWELHPSFDIVVNCSGLGSRQLAGDSKIFPVRGQVLQVQAPWVE 212
SP|Q99489-2|OXDD_HUMAN -IKGSGGWTLTRRIEDLWELHPSFDIVVNCSGLGSRQLAGDSKIFPVRGQVLQVQAPWVE 153
SP|Q99489-3|OXDD_HUMAN RIKGSGGWTLTRRIEDLWELHPSFDIVVNCSGLGSRQLAGDSKIFPVRGQVLQVQAPWVE 240
                         ************************************************************

SP|Q99489|OXDD_HUMAN   HFIRDGSGLTYIYPGTSHVTLGGTRQKGDWNLSPDAENSREILSRCCALEPSLHGACNIR 272
SP|Q99489-2|OXDD_HUMAN HFIRDGSGLTYIYPGTSHVTLGGTRQKGDWNLSPDAENSREILSRCCALEPSLHGACNIR 213
SP|Q99489-3|OXDD_HUMAN HFIRDGSGLTYIYPGTSHVTLGGTRQKGDWNLSPDAENSREILSRCCALEPSLHGACNIR 300
                        ************************************************************

SP|Q99489|OXDD_HUMAN   EKVGLRPYRPGVRLQTELLARDGQRLPVVHHYGHGSGGISVHWGTALEAARLVSECVHAL 332
SP|Q99489-2|OXDD_HUMAN EKVGLRPYRPGVRLQTELLARDGQRLPVVHHYGHGSGGISVHWGTALEAARLVSECVHAL 273
SP|Q99489-3|OXDD_HUMAN EKVGLRPYRPGVRLQTELLARDGQRLPVVHHYGHGSGGISVHWGTALEAARLVSECVHAL 360
                        ************************************************************

SP|Q99489|OXDD_HUMAN   RTPIPKSNL 341
SP|Q99489-2|OXDD_HUMAN RTPIPKSNL 282
SP|Q99489-3|OXDD_HUMAN RTPIPKSNL 369
                        *********
```

Supplementary Table 1. Procedures and conditions for hDASPO_369 inclusion bodies solubilization and refolding.

Column-based procedure:

Conditions	**1**	**2**	**3**	**4**
IB solubilization	Solubilization buffer	Solubilization buffer	Solubilization buffer + 10 µM FAD	Solubilization buffer
Column wash	Wash buffer (20 mM imidazole)	Wash buffer (5 mM imidazole)	Wash buffer (5 mM imidazole) + 10 µM FAD	
Refolding	Refolding buffer (20 mM imidazole)	Refolding buffer (5 mM imidazole)	Refolding buffer (5 mM imidazole)	Refolding buffer (5 mM imidazole)
Elution	Elution buffer	Elution buffer	Elution buffer	Elution buffer

Dialysis-based procedure:

Conditions	**1**	**2**	**3**
IB solubilization	Solubilization buffer (1 mM 2-mercaptoethanol) + 40 µM FAD	Solubilization buffer (5 mM 2-mercaptoethanol) + 40 µM FAD	50 mM Tris-HCl pH 8.0, 2 M urea, 6 M *n*-propanol, 40 µM FAD
buffer 1	20 mM Tris–HCl pH 8.0, 4 M guanidine hydrochloride, 0.5 M NaCl, 5 mM Na/K tartrate, 1 mM 2-mercaptoethanol, 40 µM FAD	20 mM Tris–HCl pH 8.0, 4 M guanidine hydrochloride, 0.5 M NaCl, 5 mM Na/K tartrate, 5 mM 2-mercaptoethanol, 40 µM FAD	20 mM Tris–HCl pH 8.0, 2 M urea, 4 M *n*-propanol, 0.25 M NaCl, 5 mM Na/K tartrate, 1 mM 2-mercaptoethanol, 40 µM FAD
buffer 2	20 mM Tris–HCl pH 8.0, 2 M guanidine hydrochloride, 0.25 M NaCl, 5 mM Na/K tartrate, 1 mM 2-mercaptoethanol, 40 µM FAD	20 mM Tris–HCl pH 8.0, 2 M guanidine hydrochloride, 0.25 M NaCl, 5 mM Na/K tartrate, 5 mM 2-mercaptoethanol, 40 µM FAD	20 mM Tris–HCl pH 8.0, 2 M urea, 2 M *n*-propanol, 0.25 M NaCl, 5 mM Na/K tartrate, 1 mM 2-mercaptoethanol, 40 µM FAD
buffer 3	20 mM Tris–HCl pH 8.0, 1 M guanidine hydrochloride, 0.1 M NaCl, 5 mM Na/K tartrate, 1 mM 2-mercaptoethanol, 40 µM FAD	20 mM Tris–HCl pH 8.0, 1 M guanidine hydrochloride, 0.1 M NaCl, 5 mM Na/K tartrate, 200 mM arginine, 350 µM oxidized glutathione, 5 mM 2-mercaptoethanol, 40 µM FAD	20 mM Tris–HCl pH 8.0, 2 M urea, 0.25 M NaCl, 5 mM Na/K tartrate, 1 mM 2-mercaptoethanol, 40 µM FAD
buffer 4	20 mM Tris–HCl pH 8.0, 0.5 M guanidine hydrochloride, 0.1 M NaCl, 5 mM Na/K tartrate, 1 mM	20 mM Tris–HCl pH 8.0, 0.5 M guanidine hydrochloride, 0.1 M NaCl, 5 mM Na/K tartrate, 200 mM arginine, 350 µM	20 mM Tris–HCl pH 8.0, 1 M urea, 0.25 M NaCl, 5 mM Na/K tartrate, 1 mM 2-mercaptoethanol, 40 µM FAD

	2-mercaptoethanol, 40 µM FAD	oxidized glutathione, 5 mM 2-mercaptoethanol, 40 µM FAD	
buffer 5	20 mM Tris–HCl pH 8.0, 0.1 M NaCl, 5 mM Na/K tartrate, 5% glycerol, 1 mM 2-mercaptoethanol, 40 µM FAD	20 mM Tris–HCl pH 8.0, 0.1 M NaCl, 5 mM Na/K tartrate, 5% glycerol, 5 mM 2-mercaptoethanol, 40 µM FAD	20 mM Tris–HCl pH 8.0, 0.25 M NaCl, 5 mM Na/K tartrate, 5% glycerol, 1 mM 2-mercaptoethanol, 40 µM FAD
buffer 6	20 mM Tris–HCl pH 8.0, 0.1 M NaCl, 10% glycerol, 1 mM 2-mercaptoethanol, 10 µM FAD	20 mM Tris–HCl pH 8.0, 0.1 M NaCl, 10% glycerol, 5 mM 2-mercaptoethanol, 10 µM FAD	20 mM Tris–HCl pH 8.0, 0.1 M NaCl, 10% glycerol, 1 mM 2-mercaptoethanol, 10 µM FAD

Solubilization buffer: 20 mM Tris-HCl pH 8.0, 6 M guanidine hydrochloride, 0.5 M NaCl, 5 mM imidazole, 1 mM 2-mercaptoethanol.
Wash buffer: 20 mM Tris-HCl pH 8.0, 6 M urea, 0.5 M NaCl, 20 mM imidazole, 1 mM 2-mercaptoethanol.
Refolding buffer: 20 mM Tris-HCl pH 8.0, 0.5 M NaCl, 20 mM imidazole, 1 mM 2-mercaptoethanol, 40 µM FAD.
Elution buffer: 20 mM Tris–HCl pH 8.0, 0.5 M NaCl, 500 mM imidazole, 1 mM 2-mercaptoethanol, 40 µM FAD.
For the column-based procedure, inclusion bodies derived from 500 mL of starting culture were resuspended in 20 mL of solubilization buffer; while for the dialysis-based procedure inclusion bodies derived from 150 mL of starting culture were resuspended in 10 mL of solubilization buffer. In the latter case, after solubilization the protein was dialyzed at 4 °C, in 500 mL of the indicated buffers, for 90 min (buffers 1-5) and overnight (buffer 6).

Supplementary Table 2. Bioinformatics prediction of protein solubility for hDASPO isoforms.

Software	Value	Score		Website	Reference
		hDASPO_341	hDASPO_369		
Protein-sol	Predicted scaled solubility	0.208	0.163	https://protein-sol.manchester.ac.uk/	Hebditch M, Carballo-Amador MA, Charonis S, Curtis R, Warwicker J. Protein-Sol: a web tool for predicting protein solubility from sequence. *Bioinformatics*. 2017;33(19):3098-3100. doi:10.1093/bioinformatics/btx345
Recombinant protein solubility prediction	Chance of solubility when overexpressed in *E. coli*	97.9%	0.0%	http://www.biotech.ou.edu/	Diaz AA, Tomba E, Lennarson R, Richard R, Bagajewicz MJ, Harrison RG. Prediction of protein solubility in Escherichia coli using logistic regression. *Biotechnol Bioeng*. 2010;105(2):374-383. doi:10.1002/bit.22537
Scratch (SOLpro)	Predicted solubility upon overexpression (probability)	0.910402	0.661469	http://scratch.proteomics.ics.uci.edu/	Magnan CN, Randall A, Baldi P. SOLpro: accurate sequence-based prediction of protein solubility. *Bioinformatics*. 2009;25(17):2200-2207. doi:10.1093/bioinformatics/btp386
SoluProt	Solubility	0.319	0.265	https://loschmidt.chemi.muni.cz/solup	Hon, J., Marusiak, M., Martinek, T., Zendulka J., Bednar, D., Damborsky, J., (2020) SoluProt: prediction of soluble expression from protein sequence. *Bioinformatics* (in preparation)

Supplementary Table 3. Primers used for cloning human hDASPO_341 and hDASPO_369 cDNA in the pcDNA3 mammalian expression vector and in the pET11a prokaryotic expression vector. Sequences recognized by the indicated endonucleases are underlined. In bold is reported the sequence encoding for the 3XFLAG peptide.

Oligo	**Sequence**	**Cloning site**
3XFLAG hDASPO 341_for	5'-ACAGCGGGATCCCACC**ATGGATTACAAGGATGACGACGATAAGGACTATAAGGACGATGATGACAAGGACTACAAAGATGATGACGATAAAC**TCGACACAGCACGGATTGCAGTTGTCG-3'	BamHI
3XFLAG hDASPO 369_for	5'-ACAGCGGGTACCCACC**ATGGATTACAAGGATGACGACGATAAGGACTATAAGGACGATGATGACAAGGACTACAAAGATGATGACGATAAAC**TCAGACCAGCCAGGCACTGGGAAACAAG-3'	KpnI
3XFLAG hDASPO 341/369_rev	5'-ACAGCGGCGGCCGCCTACAGGTTTGACTTGGGAATGGGGG-3'	NotI
pET11_hDASPO369_for	5'-GTCTACATATGCACCATCACCATCATCACATGC-3'	NdeI
pET11_hDASPO369_rev	5'-CTGTTGGATCCTCATTACAGGTTTGATTTGGGAATCG-3'	BamHI

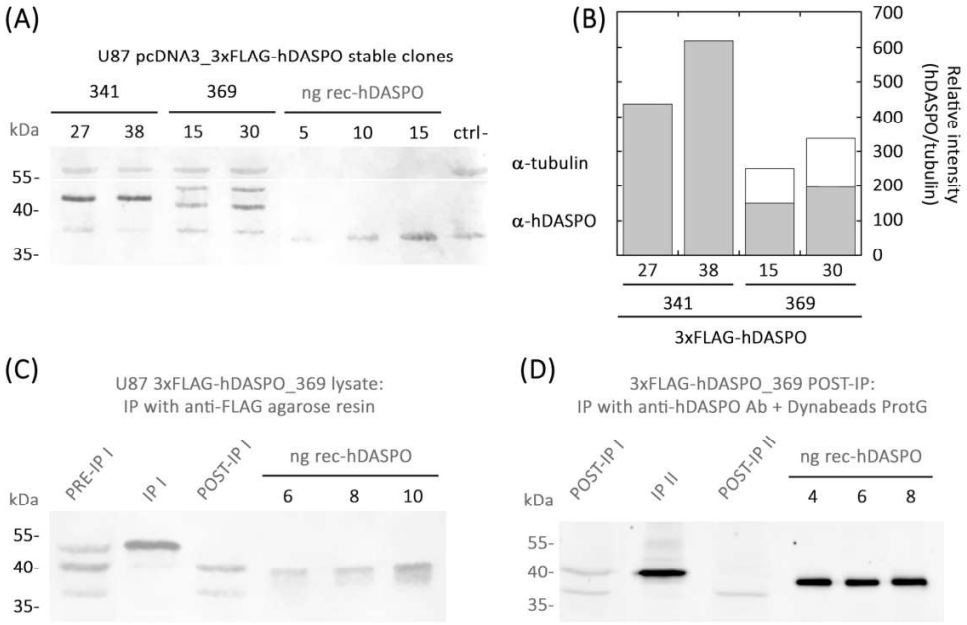

Fig. 1

165x109mm (300 x 300 DPI)

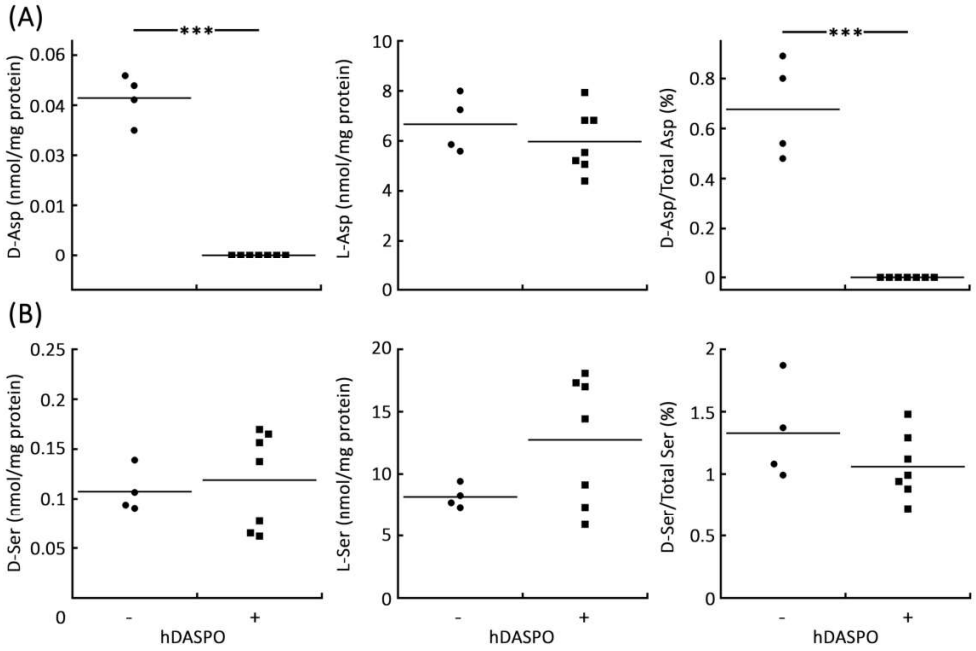

Fig. 2

165x109mm (300 x 300 DPI)

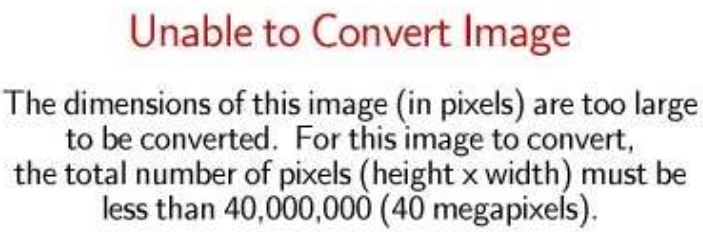
Unable to Convert Image
The dimensions of this image (in pixels) are too large
to be converted. For this image to convert,
the total number of pixels (height x width) must be
less than 40,000,000 (40 megapixels).

Fig. 3

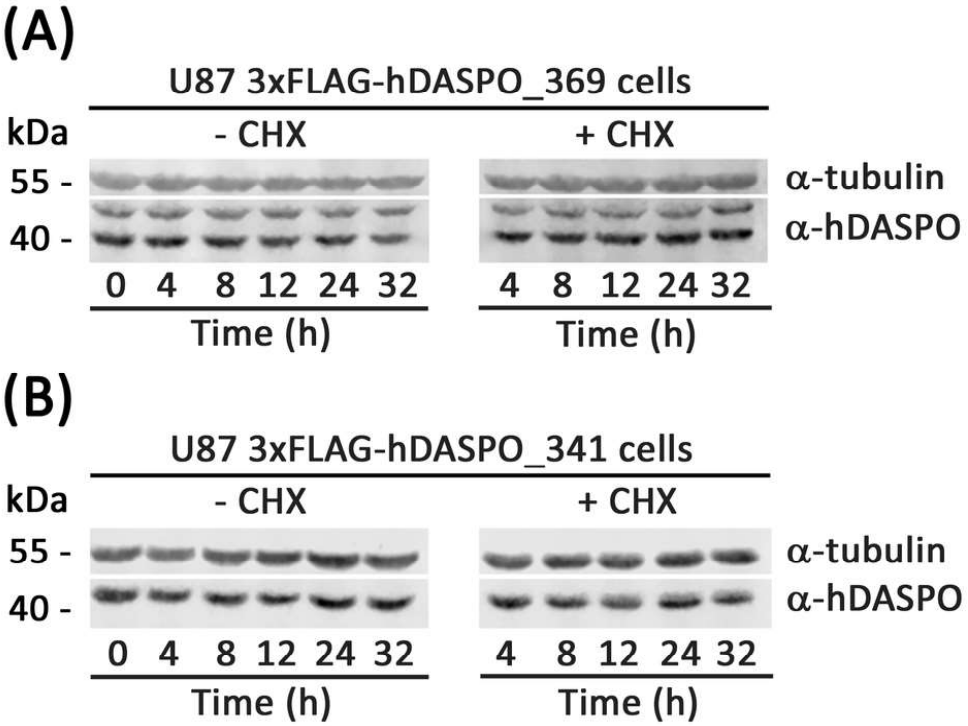

Fig. 4

79x59mm (300 x 300 DPI)

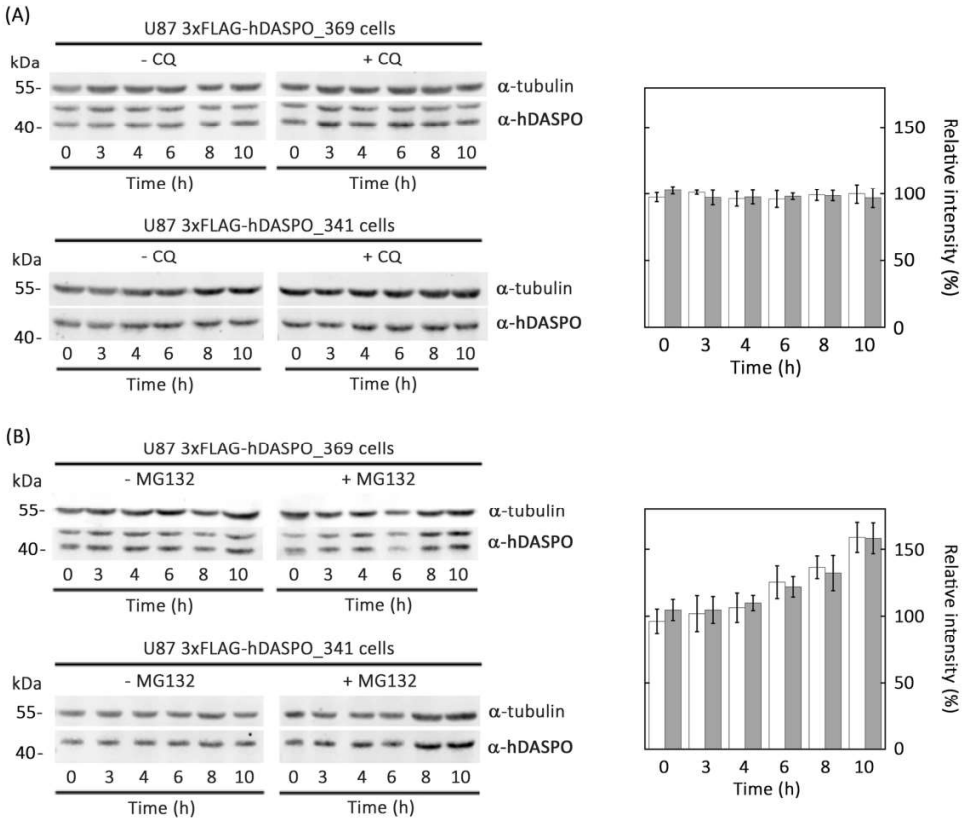

Fig. 5

165x139mm (300 x 300 DPI)

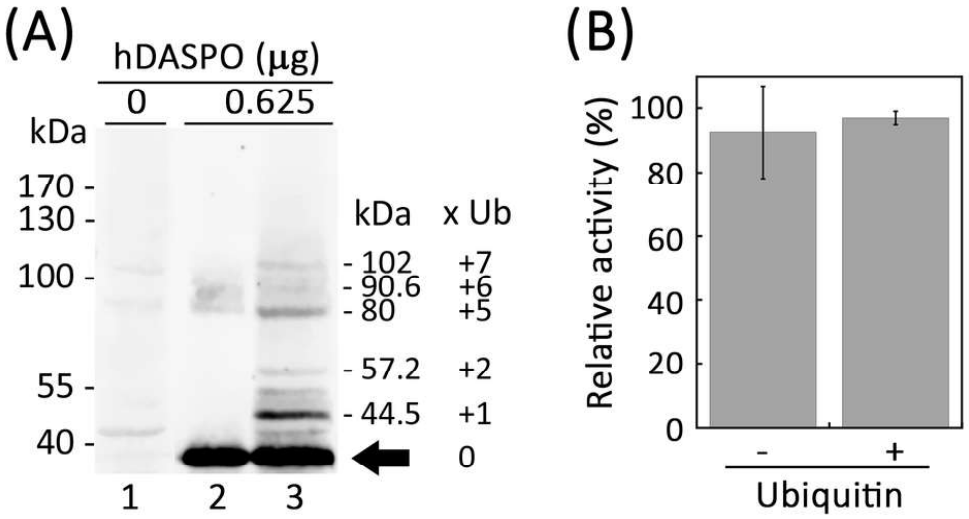

Fig. 6

80x43mm (300 x 300 DPI)

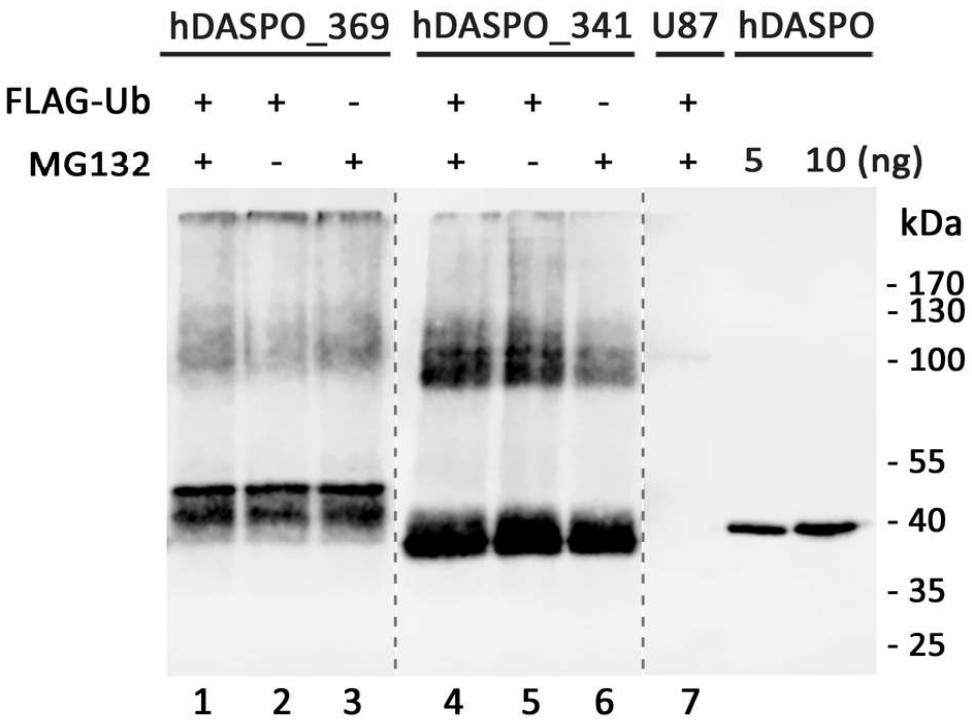

Fig. 7

80x61mm (300 x 300 DPI)